Preliminary Feasibility Study

South Cass Lake
Leak Site

Prepared for

Enbridge LLC

July 2005

Preliminary Feasibility Study

South Cass Lake Leak Site

Wenck File #0057-57

Prepared for:

Enbridge LLC
119 North 25th Street East
Superior, WI 54880-5247

Prepared by:

WENCK ASSOCIATES, INC.
360 North Robert Street
Saint Paul, MN 55101
(651) 228-1909
fax (651) 228-1969

July 2005

Wenck

Table of Contents

1.0 Introduction

Wenck Associates, Inc. (Wenck) was retained by Enbridge Energy LLC (Enbridge) to evaluate remedial options for the South Cass Lake Pumping Station Site (Site). Figure 1 shows the Site location. Natural Resources Engineering Company (NREC) previously completed a Remedial Investigation and Feasibility Study in 2003. Wenck's present involvement is to re-evaluate the remedial options for the Site. The LLBO Department of Resource Management (DRM) has jurisdiction over the Site. This report is part of a series of measures being undertaken by Enbridge in a cooperative approach with the LLBO DRM.

Of primary concern at the Site is the presence of an estimated 48,000 gallons of light non-aqueous phase liquid (LNAPL) in the surficial aquifer at the Site. Figure 2 shows the Site details and the location of the LNAPL. In this case, the term 'LNAPL' describes a body of crude oil that is present as "floating" product on the uppermost water table at the Site. The source of the oil was from a leaking flange, and possibly historical release, which was discovered by Enbridge's routine leak detection program. Additional details are presented in the NREC Remedial Investigation and Feasibility Study reports.

In general, LNAPL is a term-of-art for any lighter than water free product present as a separate phase in an aquifer. The LNAPL is distinct from the contaminant plume, which is the term used to describe contaminants that are dissolved in the groundwater and move along with the natural groundwater flow. Appendix A presents some background materials describing these terms and concepts in more detail. Throughout this report the term LNAPL, free product, or oil may be interchanged depending on the context but generally have the same meaning.

The first purpose of this report is, to re-evaluate the overall feasibility of *in-situ* remedial options for the LNAPL at the Site, to review the current state-of-the art scientific information regarding

clean up methods, and to discuss risk evaluation at petroleum contamination sites. *Ex-situ* remedies (i.e. excavation and off-Site disposal or treatment) are being evaluated separately by Enbridge. The second purpose of this report is to identify any additional information or fieldwork potentially necessary to complete a more detailed Feasibility Study. As such, this document is strategic in nature and the analysis is limited to the available data.

1.1 APPLICABLE REMEDIAL TECHNOLOGIES

The NREC feasibility study identified and described a range of remedial options for the site. These were:

- Natural Attenuation
- Crude Oil Recovery Technologies (active and passive oil skimming devices)
- Increased Oil Mobility Technologies (surfactants, thermal treatment)
- Plume Stabilization (sheet-piling wall, interceptor trench)
- Enhanced Biological Degradation (ORC - Oxygen Release Compound™)

The range of remedial options identified by NREC represents the typical range of technologies currently available for remediation of petroleum LNAPLs. Of the removal technologies, those involving skimmers and thermal treatment were the most likely to be applicable at the Site. Surfactants pose regulatory problems in Minnesota and are not generally in use at petroleum Sites in the US. NREC concluded that removal technologies were not feasible and recommended installing an impermeable barrier into the upper part of the aquifer to form a "dam" to prevent the NAPL mass from migrating.

The selection of the impermeable barrier was based on calculations of oil movement of approximately 0.5 feet per year under the natural hydraulic gradient and groundwater flow velocities present at the Site. Wenck believes that this portion of NREC's conclusions over estimate mobility of the oil body, as will be discussed and modeled below.

1.2 RISK FACTORS

The Site presents a very low risk of exposure to nearby populations or ecological receptors. The extent of both the LNAPL and the dissolved plume are well understood. There are no drinking water wells within the impacted or expected impact area. There is no present or expected discharge of oil or dissolved contaminants to any surface water body. And, importantly, the monitoring well network is sufficient to provide early evidence of any unexpected movement of oil or dissolved contaminants.

2.0 Modeling of Oil Mobility

To evaluate the range of in-situ remedial options it is first necessary to assess the overall mobility of the LNAPL. The available technologies involve mobilizing the LNAPL into wells or subsurface collection trenches for removal. Therefore, a critical aspect of evaluating any of the applicable technologies is the mobility of the oil in the subsurface and, moreover, the success of any technology depends on the extent to which the oil can be moved. Furthermore, the potential risk posed by the LNAPL is also based on the extent to which the oil may move toward receptors in the future. So, prior to approaching a detailed analysis of removal technologies, an assessment of the mobility of the oil under a variety of conditions must be completed.

2.1 BACKGROUND ON LNAPL MOBILITY

The aquifer system at the Site, as is typical at all sites with LNAPL, is a complex flow regime including three fluid phases: air, water, and oil. The mobility of LNAPL depends on a number of variables including fluid viscosities, interfacial tensions, wetting versus non-wetting fluids and the oil/water saturation, among others. Calculating the mobility and movement of LNAPL in a three-phase system requires computer simulations to perform the calculations. Fortunately, due the presence of large numbers of similar Sites across the US and Europe (thousands of sites since the 1980's) extensive research has been conducted and relatively simple spreadsheet-based computer models have been recently developed that closely approximate the more complex computer models. This large body of research and practical experience has also resulted in a well-understood body of knowledge about the long-term effectiveness of remedial technologies and the behavior of LNAPL problems over time.

In general, the oil is less mobile as viscosity and interfacial tension increases. In addition, the relative permeability of the aquifer to oil movement is highly dependent on the oil/water

saturation. The aquifer has a maximum permeability to oil at full saturation (100% oil). As the percentage of oil is reduced, the permeability of the aquifer to oil is reduced. Ultimately, for any set of oil properties, there is a "residual saturation" below which the mobility of the oil is essentially zero. This behavior poses advantages and disadvantages to remediating the Site.

First, the existence of a residual saturation means that there is a limit to how much oil can be removed by a given technology. Enhancing the oil mobility via heat, for example, can serve to reduce the residual saturation and improve the removal but there is always remains a significant residual saturation of LNAPL.

Second, however, this behavior results in LNAPL bodies being highly stable or immobile in most situations. Typically, after a release, the oil spreads out on the surface of the aquifer and penetrates downward under gravity. At first the oil is near its maximum mobility, since it exists as nearly 100% oil and continues to spread. As the oil spreads along and into the aquifer it intermingles with the water and soil grains. As the oil spreads out the ratio of oil to water decreases. The water and oil share space within the soil matrix and the interfacial tension between the two fluids reduces the mobility of the oil. As this ratio decreases, the oil reaches its residual saturation and becomes immobile. Eventually, the oil forms individual "blobs" and "ganglia" that are surrounded by water and remain attached to the soil grains by surface tension. In this situation the oil remains immobile unless there are additional spills to drive more oil outward from the source area. The typical situation arises when there is a fringe of oil at residual saturation surrounding a central core of higher oil saturation that no longer has enough mobility to spread further.

What this means, and has been observed at many sites over decades, is that petroleum LNAPL bodies (particularly heavy oils) tend to become stable and do not migrate under the normal flow of groundwater. Movement only occurs when there is a continuing source of oil (ongoing leaks or spills) to provide a driving force to keep the oil spreading. In these cases the primary concern becomes the dissolved plume that forms downgradient of the stable LNAPL body.

3.0 Spread Sheet Modeling of LNAPL

The American Petroleum Institute has developed a series of computer spread-sheet based models to assist is assessing the mobility of LNAPL at petroleum spill sites (*"Models for Design of Free-Product Recovery Systems for Petroleum Hydrocarbon Liquids," Regulatory Analysis and Scientific Affairs Department, Pub. No. 4729, American Petroleum Institute, August 2003*). These models are available at the API Web Site: (http://groundwater.api.org/lnaplguide/index.cfm).

These models permit calculations of the effectiveness using extraction wells or trenches to remove oil based on site-specific inputs of aquifer properties and LNAPL properties. Both field data and generic data can be used for inputs, depending on what is available for the site.

Fortunately, the South Cass Lake database included measurements of oil thickness, and viscosity at several temperatures at a number of wells. In addition, the aquifer permeability and gradient have been measured. The database is nearly ideal for using the spreadsheet models.

3.1 SIMULATIONS

Table 1 presents the oil properties used as input data used for the modeling. The data were obtained from the latest monitoring data provided by Enbridge (April 2005 monitoring event). The data represent the range of oil properties observed at the Site, including viscosity measurements at three temperatures ranging from 10°C to 30°C.

Two sets of model runs were prepared and are presented in Appendix B. First are a set of runs representing the data from MW5, where the thickest oil accumulation and the highest viscosities were measured. The second set was at MW13 where the oil accumulation is thinner and the

viscosities an order of magnitude less. These simulations represent the range of conditions that exist at the Site. Figure 2 presents the well locations and LNAPL extent for reference.

For the MW5 data, runs simulating a typical extraction well, a typical extraction trench and a vacuum enhanced well were completed. In addition, the model was run with the oil viscosity at 30°C to simulate the addition of heat to the aquifer. For MW13 the same runs were made, except for the trench, since the trench simulation for MW5 data essentially represents the best case for removing the entire LNAPL body using trench technology.

The aquifer properties were taken from the remedial investigation work. Other oil properties such as interfacial tension and density were taken from tables of generic data for crude oil included with the spreadsheet documentation.

3.2 MW5 EXTRACTION WELL MODEL RUNS

Appendix B.1 contains the results of the model runs on the MW5 data. Each portion of the run is separated in Appendix B.1 to aid in following the discussion. Table 2 presents a summary of all the runs. An initial thickness of 1.09 feet of oil was used as the starting condition, with dynamic viscosity of 378 centipoise (cp). The first section of the run shows the input data, calculations of relative permeability and saturation, and generic data used as input. The sheets labeled "Free Product Recover System Analysis" shows the predicted behavior of a LNAPL extraction well. These runs reflect a single well with an estimated radius of influence of 30 feet. A full-scale system would involve roughly 5 to 10 similar wells.

MW5 Water Enhanced Recovery:

In this case a pumping rate of 5 gpm was estimated based on experience at similar sites. As the first graph shows, the LNAPL thickness around the extraction well would be reduced from 1.09 feet to approximately 0.72 feet over a 5-year period. The second graph shows that approximately 842 gallons of product would be recovered out of 3000 gallons within the 30-foot radius of capture of the well, or roughly 28% of the total oil present. And the third graph shows that LNAPL production would drop from 0.82 to 0.26 gallons per day by the fifth year of operation. All three graphs show diminishing performance over the 5-year period. Here are the excerpted graphs:

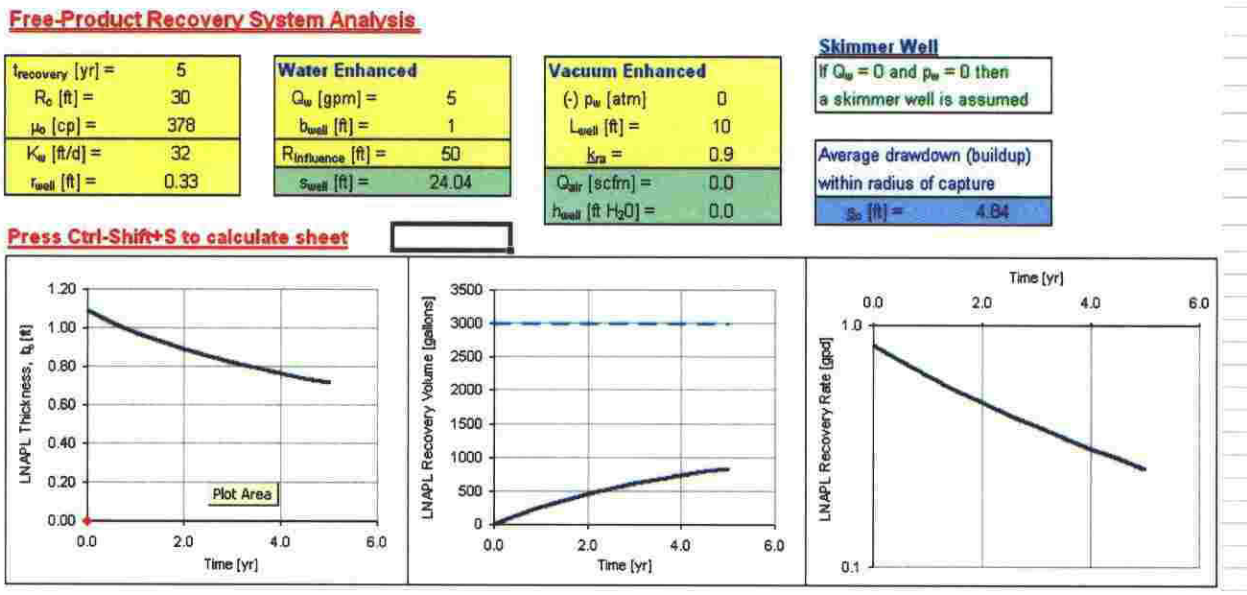

MW5 Vacuum Enhanced Recovery:

The next graph shows the addition of vacuum enhancement to the system. An aggressive 1 atm suction head is applied to the well. The removal improves to some extent but the oil thickness levels out at about 0.61 feet and the oil recovery rate levels off at 0.1 gpd. The total oil removal is about 1264 gallons or about 42% of the total oil present within the radius of capture of the well. Here are the excerpted graphs:

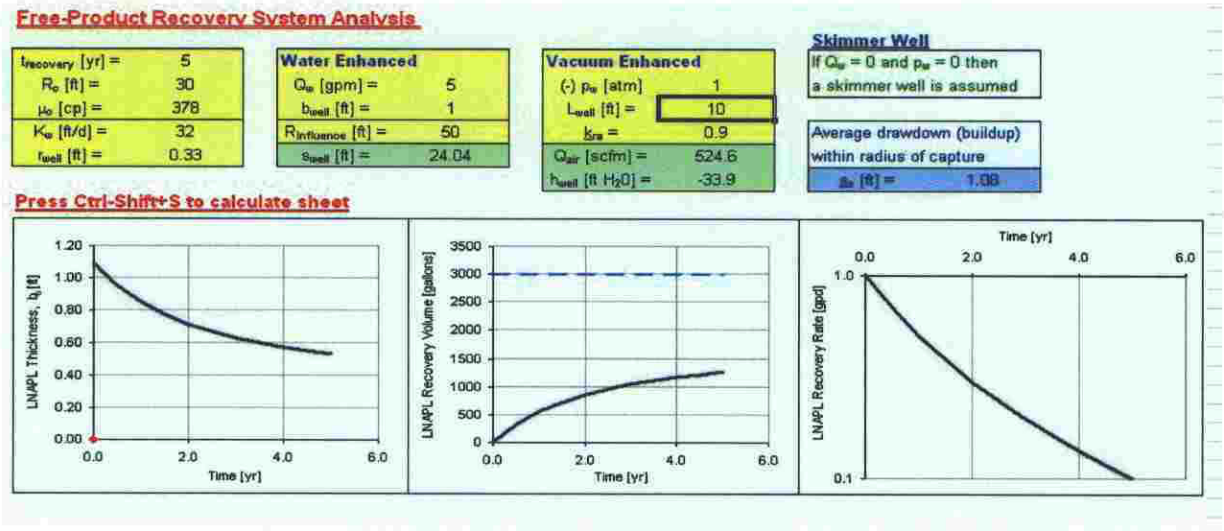

MW5 Reduced Viscosity (heat):

The third set of graphs shows the effect of an extraction well and reducing the viscosity to 101 cp, simulating a heating of the aquifer from 10°C to 30°C (it should be noted that the viscosity of the water also changes with temperature but this is beyond the capability of the software). This shows improvements similar to the application of a vacuum to the extraction well. The total oil removal is 1395 gallons, or 46%of the total within the radius of capture. The LNAPL thickness is reduced to 0.48 feet. The LNAPL production rate drops from 3 gallons per day to 0.17 gallons per day after 5 years. . Here are the excerpted

graphs:

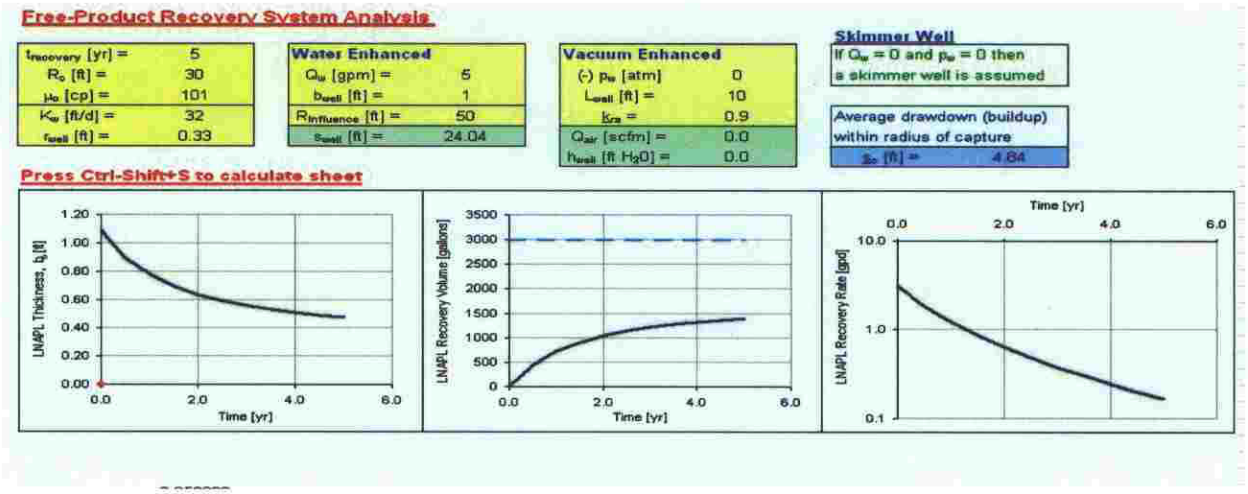

MW5 Trench Recovery:

The sheet labeled Trench Recovery Analysis shows the predicted behavior of an extraction trench over a 5-year period. This scenario consists of a simulation of a trench extraction system with a 150-foot long collection trench installed width-wise across the down gradient edge of the LNAPL zone. The trench is set to operate at 10 gpm. This scenario shows only minor reductions in both LNAPL thickness (1.09 feet to 1feet). The total oil removed is approximately 1339 gallons, out of a model predicted 30,000 gallons, or only 4% of the total. The total water pumped during this simulation was 26 million gallons. . Here are the excerpted graphs:

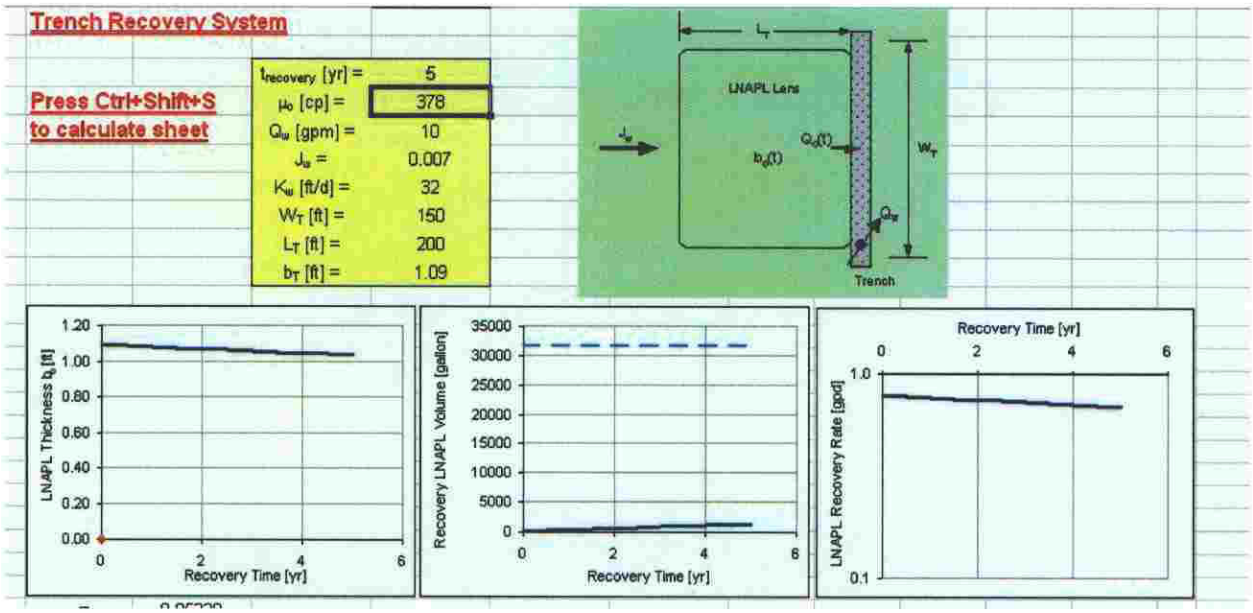

3.3 MW13 MODEL RUNS

Appendix B.2 contains the results of the model runs on the MW13 data. This simulation represents the potential oil recovery in the areas of thinner oil accumulation and lower oils viscosities, representing the fringes of the LNAPL body. An initial thickness of 0.49 feet of oil was used as the starting condition, with dynamic viscosity of 21.2 centipoise. The first page of the run shows the input data. The second and third page present calculations of relative permeability and saturation. The sheets labeled "Free Product Recover System Analysis" shows

the predicted behavior of a LNAPL extraction well These runs reflect a single well with a radius of influence of 30 feet. Multiple wells would be needed in a full-scale system.

MW13 Water Enhanced Recovery:

Similar to the MW5 simulations, a pumping rate of 5 gpm was used. As the first graph shows, the LNAPL thickness around the extraction well would be reduced from 0.49 feet to approximately 0.32 feet over a 5-year period. The second graph shows that approximately 102 gallons of product would be recovered out of 816 gallons within the radius of capture of the well, or roughly 13% of the total oil present. And the third graph shows that LNAPL production would drop from 0.1 to 0.03 gallons per day by the fifth year of operation. All three graphs show diminishing performance over the 5-year period. . Here are the excerpted graphs:

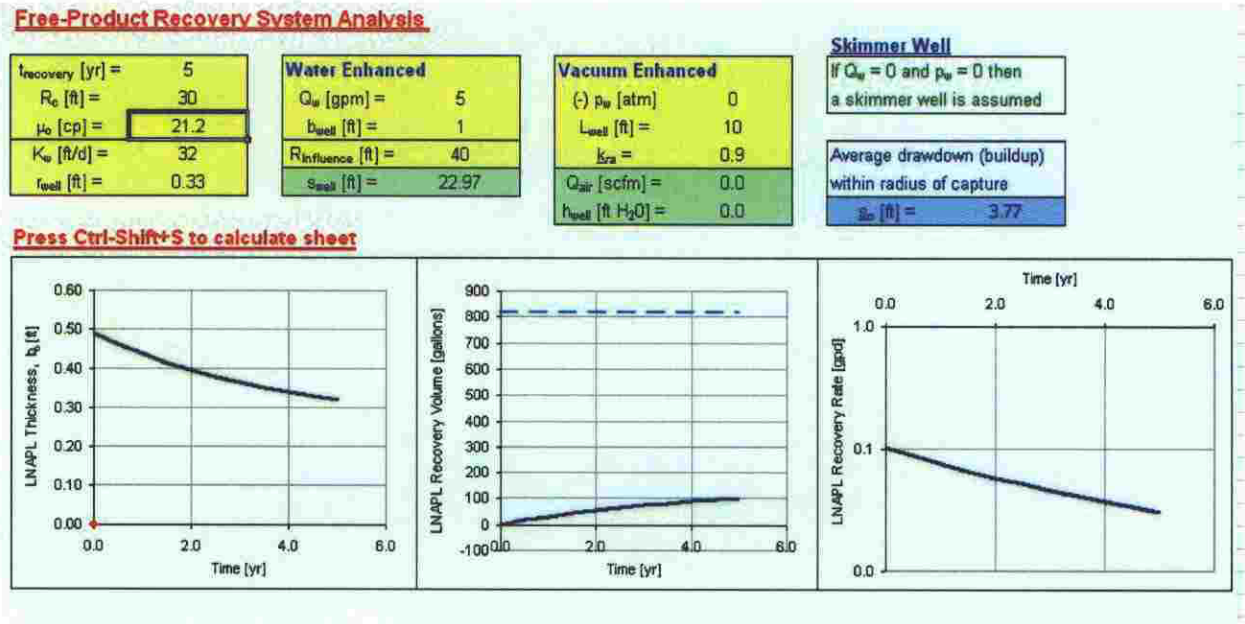

MW13 Vacuum Enhanced Recovery:

The next graph shows the addition of vacuum enhancement to the system. An aggressive 1 atm suction head is applied to the well. The removals improve to some extent but the oil thickness levels out at 0.24 feet and the oil recovery rate drops to less than levels off at 0.1 gpd. The total oil removal is about 151 gallons or about 19% of the total oil present within the radius of capture of the well. . Here are the excerpted graphs:

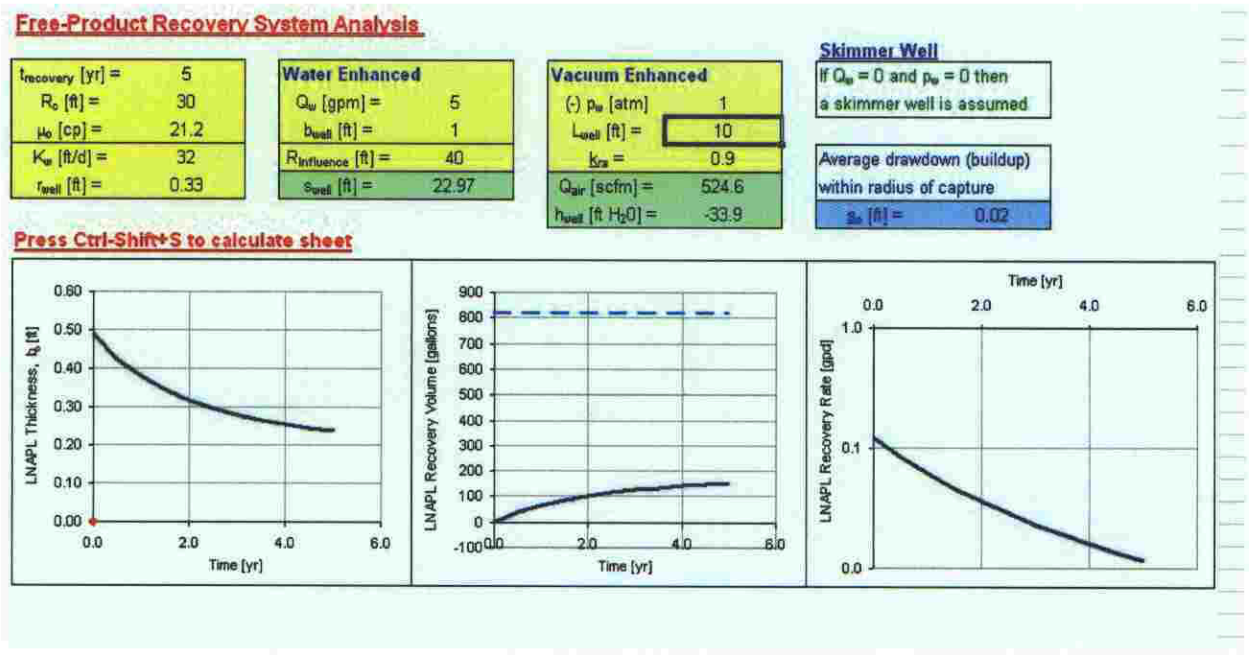

MW13 Reduced Viscosity (heat):

The third set of graphs shows the effect of an extraction well and reducing the viscosity to 9.8 cp, simulating a heating of the aquifer from 10°C to 30°C. This shows improvements similar to the application of a vacuum to the extraction well. The total oil removal is 144 gallons, or 18% the total within the radius of capture. The LNAPL thickness is reduced to 0.25 feet. The LNAPL production rate drops to 0.18 gallons per day after 5 years. . Here are the excerpted graphs:

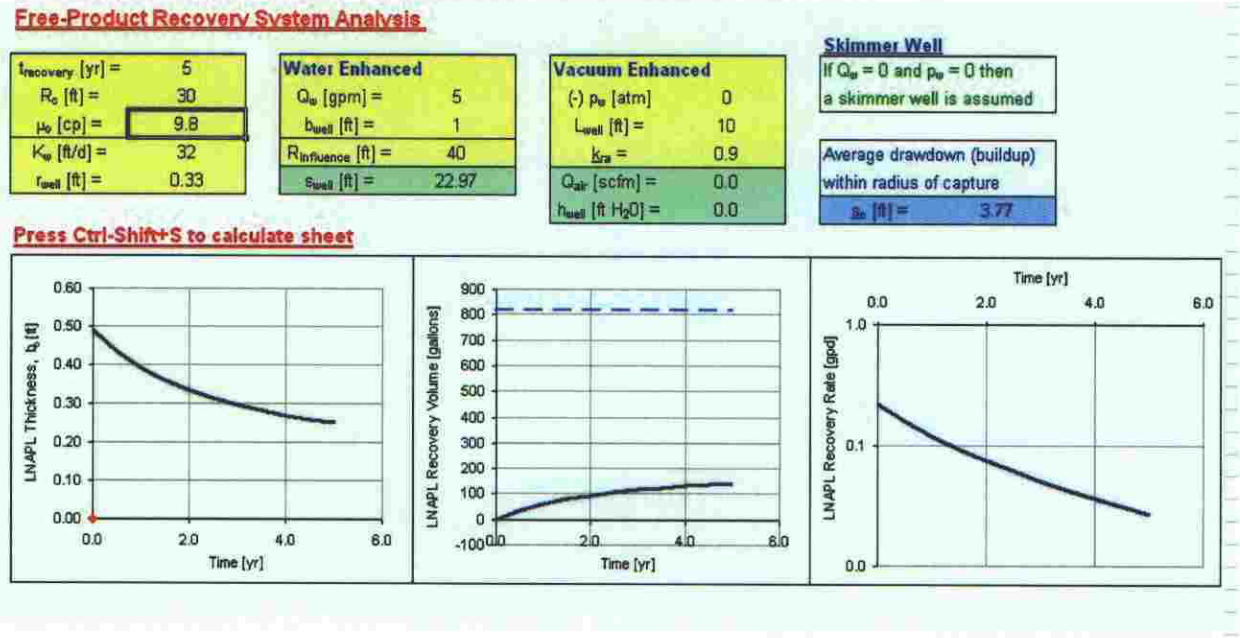

3.4 DISCUSSION OF RESULTS

Table 2 presents a summary of the simulation runs and the removal and thickness reductions possible. As these simulations show, the best estimates for recovery of LNAPL, even with application of heat or vacuum enhancement, are of 46% in the thickest accumulations and only 23% in the thinner areas of the LNAPL. This decrease in the fringes of the NAPL body reflects the fact that the relative permeability of oil is reduced as the oil to water ratio is reduced. Thus, even though the oil is significantly less viscous at MW13, the lower starting saturation results in less removal on a percentage basis. This is the typical behavior at LNAPL sites, discussed in section 2.1, where there is a fringe of oil at residual saturation surrounding a central core of higher oil saturation that no longer has enough mobility to spread further.

Assuming that roughly 1/3 of NAPL plume is represented by the data at MW5 and 2/3 is represented by MW13, the model results show that enhanced recovery efforts using wells (either vacuum or heat enhanced) would likely remove on the order of 28% of the LNAPL over a 5-year period. Closer inspection of the model runs show that the efficiency of removal generally begins dropping significantly after 2 years.

For the scenarios based on wells, the water removed (and treated) during these simulations equates to 13 million gallons per well over the 5-year simulation. For the estimated 5 to 10 wells necessary to complete such a remedy the total water needing extraction, treatment and discharge would be 65 million to130 million gallons. The multiple wells necessary to complete such a system would increase this volume accordingly. The trench scenario would involve removing, treating and disposing of 26 million gallons of water.

4.0 Exposure Pathway Discussion

The question becomes, does removing 28% of the oil reduce the short or long term risks at the Site? The subject of source area reductions at petroleum LNAPL sites has been the subject of much discussion in the petroleum remediation industry. One of the more complete discussions is contained in a 2002 paper by David Huntley, et al. of the University of San Diego entitled: "Persistence of LNAPL Sources: Relationship between Risk Reduction and LNAPL Recovery." A copy of the paper is presented in Appendix C.

Huntley found that, except for coarse-grained soils (sand and gravel) or very thick accumulations of LNAPL there is not a significant reduction in risk associated with removing a portion of the LNAPL (as the above simulations show are technically possible). This seems counter intuitive.

To understand the basis for this finding, the bio-geochemistry of the dissolved plume needs to be taken into account. What the research shows is that dissolved plumes of benzene, toluene, ethyl benzene and xylenes (commonly called BTEX) associated with petroleum LNAPL rapidly reach an equilibrium in terms of size and concentration. That is, these plumes reach a certain extent in the aquifer and then stop growing due to the natural breakdown of the contaminants due to biological activity in the aquifer. Petroleum compounds generally make good energy sources for aerobic bacteria, which are naturally present in an aquifer.

To simplify somewhat, what Huntley, et al. show in their paper is that the size of the BTEX plume is largely independent of the volume of LNAPL left in the source area. This can be understood when thought of in terms of solubility. The BTEX plume is usually in the parts-per billion to parts per million range. These concentrations are extremely small compared to the mass of the LNAPL. In addition the petroleum compounds have low solubility compared to the mass of product. Thus a relatively small percentage of free product is able to sustain a BTEX

plume and the limiting factor is the solubility and biological activity rather than the free product mass.

Over the long term the oil can be expected to "weather" as lighter fractions dissolve into the plume, compounds breakdown due to biological activity around the perimeter of the LNAPL, or volatilize into the overlying soil. This weathering will reduce the mobility further as the oil thickens in response to the weathering. Thus the mobility and "strength" of the LNAPL source will reduce itself over time.

The result of this and related research is that, in general, enhanced recovery efforts are not used at simple petroleum sites where there is not a direct exposure or potential exposure to the LNAPL itself. An exception may be a site with other hazardous chemicals associated with the petroleum (e.g. PCB or pentachlorphenol), which is not the case here. Typically, monitoring is used to establish that the dissolved BTEX plume is stable or shrinking and long term monitoring is used to provide ongoing confirmation that there is no exposure.

Along with monitoring, oil that accumulates in a well is removed by hand or via a passive skimmer system is as is practical. This is considered a general good practice in the remediation industry and as a matter of good housekeeping. Typically the Minnesota Pollution Control Agency requires practical recovery of NAPL that accumulates in monitoring wells. The oil removal is usually done in conjunction with the groundwater monitoring rounds.

5.0 Conclusions

- The modeling shows that, even with enhanced recovery, a maximum of approximately 28% of the oil is potentially recoverable.

- Enhanced recovery would also entail extracting and treating 65 to 130 million gallons of water over a 5-year system life span. A trench would extract 26 million gallons of water.

- There are no existing or expected human or ecological exposure pathways to the LNAPL or dissolved plume.

- Removing oil at the Site is not likely to change the nature, extent or longevity of the dissolved groundwater plume at the Site.

- The LNAPL is likely physically stable due to the lack of a continuing source and the heavy nature of the LNAPL itself (crude oil).

- An impermeable barrier is not necessary to assure physical confinement of the LNAPL.

6.0 Recommendations

Based on the results of the modeling, and the current scientific literature, and Wenck's experience the following recommendations are made:

- Continue observation of oil thickness over time to confirm physical stability of LNAPL,
- Continue groundwater monitoring to verify stability of the dissolved plume,
- Monitor natural attenuation indicators (as recommended in the NREC feasibility study),
- Evaluate manual methods or passive skimmer devices for practical recovery of oil that accumulates in wells.
- If the skimming proves effective, re-evaluate additional passive recovery methods.
- Prepare an evaluation of the natural attenuation of the dissolved plume and the physical stability of the LNAPL after two additional years of monitoring (through 2007).

TABLES

Table 1

Crude Oil Viscosity and Thickness Summary

Table 1
Crude Oil Viscosity and ThicknessSummary
Enbridge Pipelines (Lakehead), L.L.C. - South Cass Lake Station

Location	Temperature (°C)	Kinematic Viscosity (cSt)	Dynamic Viscosity (cP)	Oil Thickness (ft.)
MW-5	10	421.1	378.9	1.09
	20	206.7	186.1	
	30	112.7	101.4	
MW-11	10	82.2	74.0	0.69
	20	47.5	42.8	
	30	30.2	27.2	
MW-13	10	23.6	21.2	
	20	15.6	14.0	
	30	10.9	9.8	0.42

Notes: Thickness from April 2005 measurements
Dynamic viscosity based on density of 0.9

Table 2

Summary of Model runs

Table 2
Summary of Model Runs
Enbridge Pipelines (Lakehead), L.L.C. - South Cass Lake Station

Well	Scenario	Dynamic Viscosity (cp)	Starting LNAPL Thickness (ft.)	Ending LNAPL Thickness (ft.)	Oil Removed (Gallons)	Percentage LNAPL Removal	Starting Oil Removal Rate (gal/day)	Ending Oil Removal Rate (gal/day)
MW5	**Water enhanced recovery**	378	1.09	0.72	842	28%	0.82	0.26
MW5	**Vacuum ehanced Recovery**	378	1.09	0.6	1264	42%	1	0.1
MW5	**Reduced viscosity (heat)**	101	1.09	0.48	1395	46%	3.09	0.17
MW5	**Trench recovery**	378	1.09	1.034	1339	4%	0.79	0.69
MW13	**Water enhanced recovery**	21.2	0.49	0.32	102	13%	0.1	0.03
MW13	**Vacuum ehanced recovery**	21.2	0.49	0.24	151	19%	0.12	0.01
MW13	**Reduced viscosity (heat)**	9.8	0.49	0.25	144	18%	0.22	0.18

Note: Oil removed from well simulation reflects a single well with a capture radius of 30 feet, the trench reflects the entire NAPL body. Therefore the percentage removal reflects the area of capture only.

FIGURES

Figure 1

Site Location Map

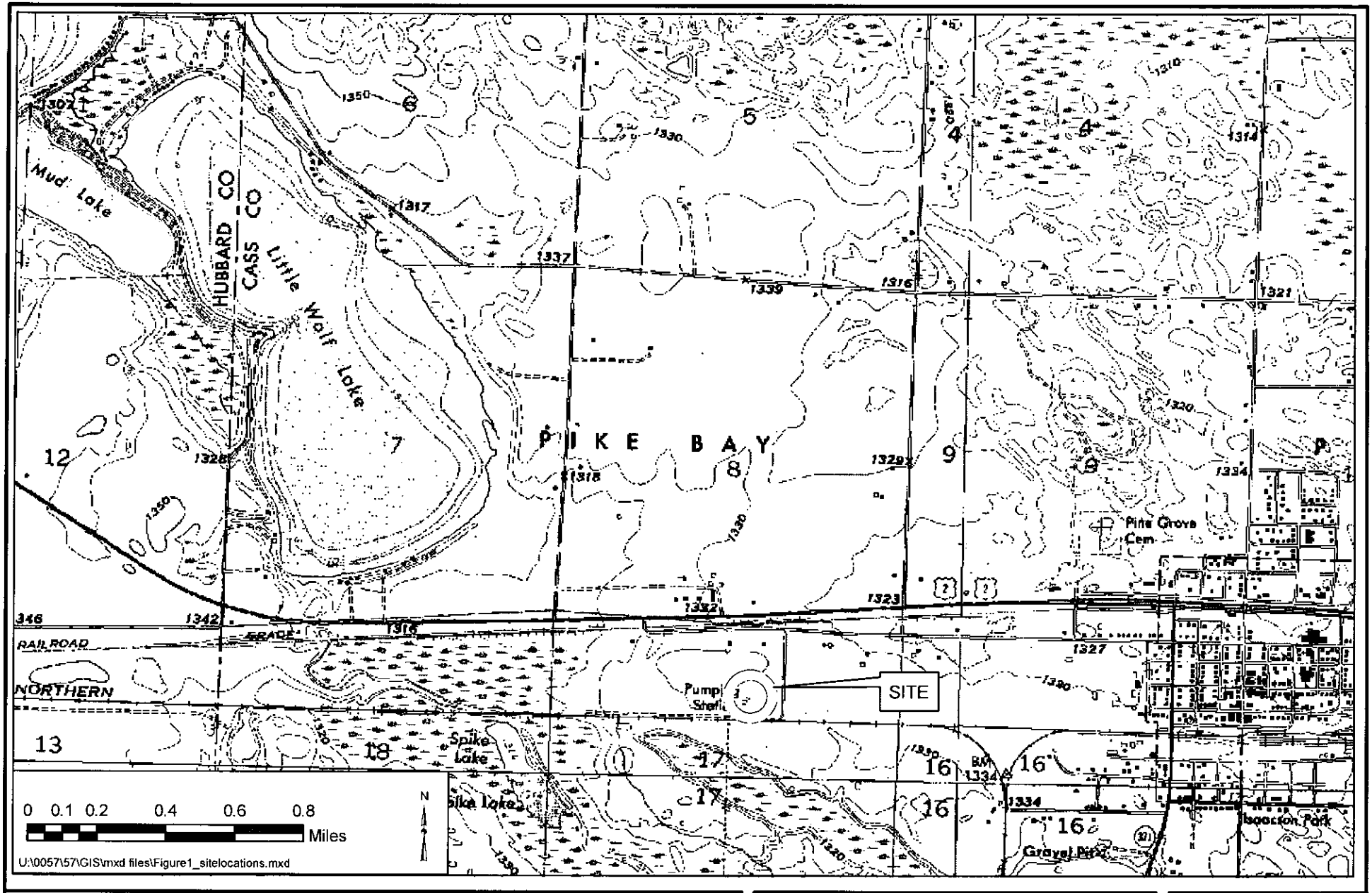

Enbridge LLC South Cass Lake Site	Wenck Associates, Inc. Environmental Engineers — Wenck — 1800 Pioneer Creek Center Maple Plain, MN 55359-0429	JUL 2005
Site Location Map		Figure 1

Figure 2

Lateral Extent of Residual Product (NAPL)

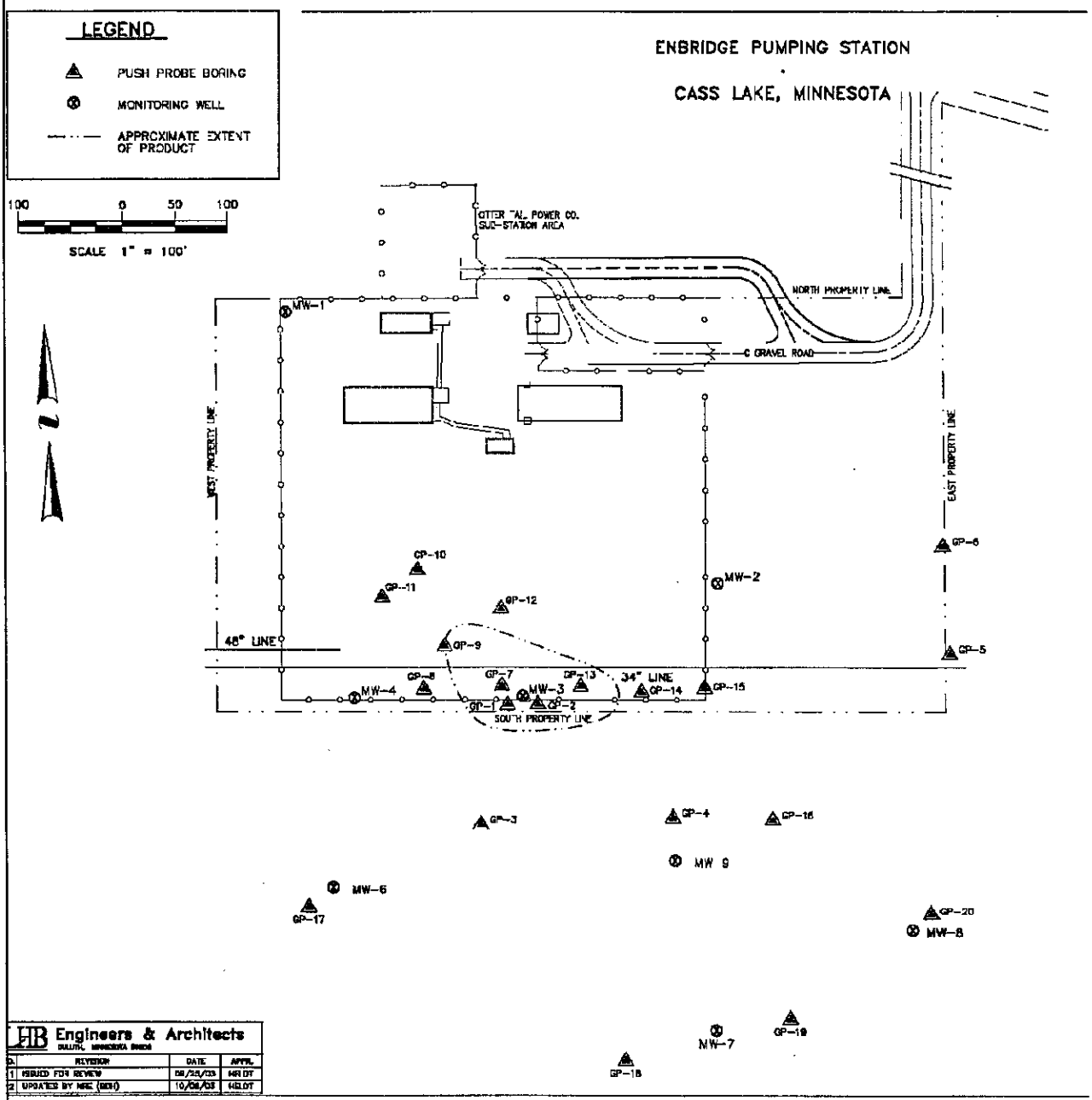

U:\0057\57\GIS\mxd files/Figure2.mxd

Enbridge LLC South Cass Lake Site	Wenck Wenck Associates, Inc. 1800 Pioneer Creek Center Environmental Engineers Maple Plain, MN 55359-0429	JUL 2005
Lateral Extent of Residual Product (NAPL)		Figure 2

APPENDIX A

Appendix A

API Interactive LNAPL Guide

American Petroleum Institute

API Interactive LNAPL Guide

Version 2.0

Prepared for:
The American Petroleum Institute's Soil and Groundwater Technical Task Force

Developed by:
Environmental Systems & Technologies
(A Division of Groundwater & Environmental Services, Inc.)
Blacksburg, Virginia

Aqui-Ver, Inc.
Park City, Utah

August 2004

ACKNOWLEDGMENTS

API STAFF CONTACT

Harley Hopkins, Regulatory Analysis and Scientific Affairs Department (RASA)

MEMBERS OF THE API SOIL AND GROUNDWATER TECHNICAL TASK FORCE

The API would like to acknowledge the following task force members for their contributions of time and expertise during this study and in the preparation of this guide:

Curtis Stanley, Shell Global Solutions (US) Inc.; (Chairman)

Mark Adamski, BP p.l.c

Tim Buscheck, ChevronTexaco Corporation

Brian Davis, ChevronTexaco Corporation

George DeVaull, Shell Global Solutions (US) Inc

Jim Higinbotham, Exxon Mobil Corporation

Tom Henson, Exxon Mobil Corporation

Dan Irvin, ConocoPhillips Company

Ravi Kolhatkar, Atlantic Richfield Company, A BP Affiliated Company

Victor Kremesec, Atlantic Richfield Company, A BP Affiliated Company

Mark Lyverse, ChevronTexaco Corporation

DEVELOPERS

The API would like to acknowledge the contributions of the following content and software developers:

Mary Ann Parcher, ES&T, a Division of GES Inc.

Pramod Thota, ES&T, a Division of GES Inc.

Don Lundy, ES&T, a Division of GES Inc.

G.D. Beckett, Aqui-Ver, Inc.

Christine Curley, Aqui-Ver, Inc.

Jeffrey Johnson, RETEC

Introduction

A nonaqueous phase liquid results from the physical and chemical differences between liquid hydrocarbon and water, such that a physical interface exists between the two liquids. Hence, nonaqueous phase liquids act as a distinct fluid within the subsurface. Nonaqueous phase liquids, which are commonly referred to by the acronym "NAPL," have typically been divided into two general categories, light and dense. These terms describe the specific gravity or the density of the NAPL with respect to water. Light nonaqueous phase liquids, termed "L"NAPLs, have a specific gravity less than water and dense nonaqueous phase liquids, termed "D"NAPLs, have a specific gravity greater than water. Examples of LNAPLs include most fuels (gasoline, diesel, jet A, heating oil) and lubricants. DNAPLs include chlorinated solvents, creosote based wood-treating oils, coal tar wastes, and pesticides. Although many of the same principles and concerns apply to both LNAPLs and DNAPLs, the focus of this guide is on LNAPLs since these compounds comprise the most common type of contaminants at petroleum retail, storage, distribution and refining sites.

LNAPL contamination poses one of the most significant issues faced by the environmental industry. In particular, LNAPL contamination has typically been perceived as a significant environmental threat by the general public and the regulatory community, and as a result, LNAPL cleanup standards are generally very conservative. Technically, the remediation of LNAPL is difficult because it is significantly influenced by the physical character of the product, the nature of the soil conditions, and the hydrologic setting. LNAPL acts as a source of volatile and dissolved contaminants that may require remediation. Additionally, if sufficient volume exists, LNAPL may migrate posing significant environmental and legal concerns. To effectively manage the various and difficult aspects of LNAPL contamination, one must conceptually and technically understand the sometimes complex issues posed by LNAPL contamination. It is only through this understanding that appropriate management decisions can be made.

The management of LNAPL contaminated sites is a scientific and an engineering challenge. The focus of this primer is to present general fundamental concepts in understanding how subsurface processes and conditions influence the movement and retention of LNAPL in the subsurface. Specifically, these processes require knowledge of chemistry, geology, hydrology, soil science, biology, and engineering. The objective of this primer will be to provide general information on key factors to consider and recognize when managing a LNAPL site. This *NAPL Basics* primer will form the basis of more technical discussions presented in other primers.

LNAPL Movement in the Subsurface

Products typically produced, stored, and distributed include gasoline, middle distillates (diesel, kerosene), and heavy fuel and lubricating oils. These products vary in chemical composition and physical properties. The characteristics of these product types in conjunction with the hydrogeologic conditions at the site and the manner in which the product is released are the primary factors that influence the movement and distribution of LNAPL in the subsurface. When oil is accidentally released at the surface or from an underground pipe or storage tank, oil migrates vertically downward under the force of gravity. When the volume of the release is sufficient, the LNAPL will migrate through the unsaturated zone to the capillary fringe and water table (Figure 1). The increasing water content in the capillary fringe and the effects of buoyancy will impede the vertical movement of the LNAPL near the water table. As a result, the less dense oil will begin to migrate laterally along the water table. In general, the lateral oil migration will preferentially flow with the water table gradient. However, if the rate of downward vertical LNAPL movement from the surface is greater than the lateral migration, the oil will begin to mound vertically and oil flow may become radial. In addition, downward migration into the aquifer will increase displacing water from the aquifer pore space.

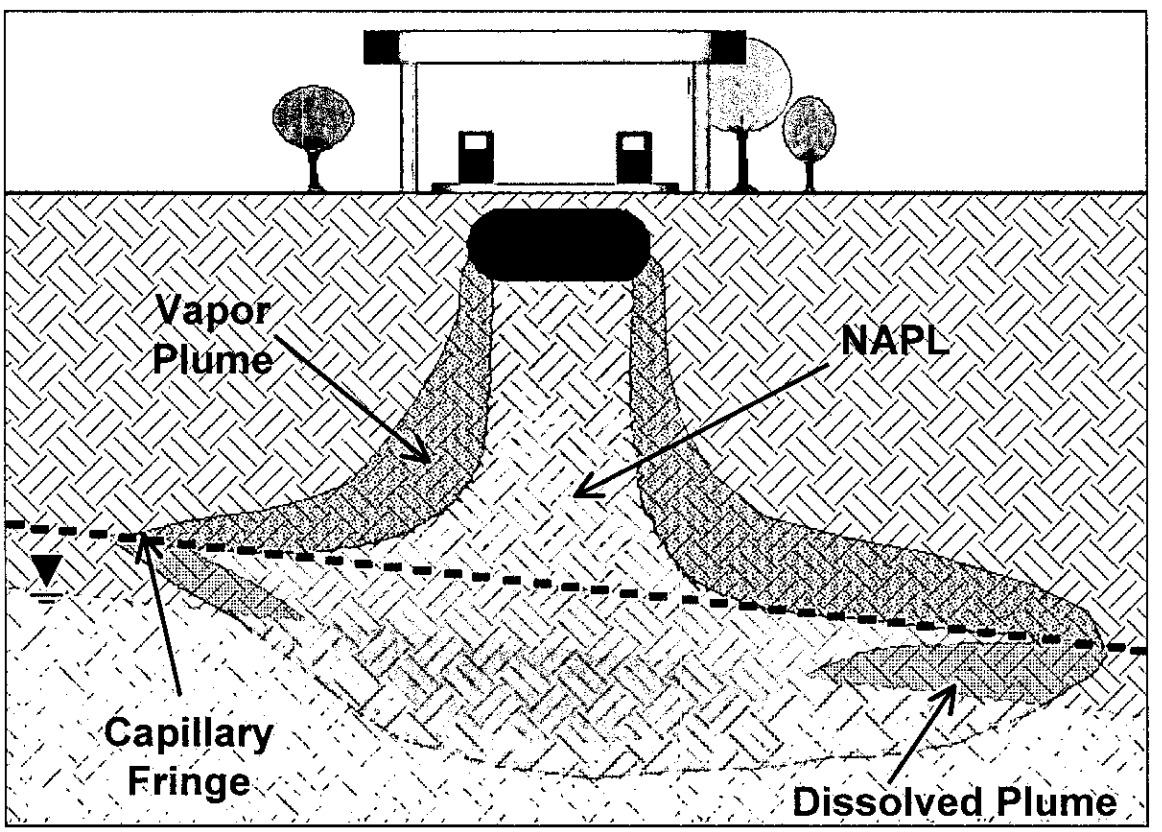

Figure 1. Representation of a LNAPL Release to the Subsurface.

In the aquifer, LNAPL coexists with water in the soil pores. The percentage of LNAPL filling the total pore space is termed the oil saturation. Due to the presence of water in the soil, LNAPL saturations are never 100 percent but may range from as little as 5 percent to over 70 percent (Figure 2). The percent saturation and distribution of LNAPL within the pore network will change over time as oil initially displaces water and is then subsequently displaced as water refills pore spaces when water levels rise.

In the past, a common misconception of the vertical distribution of free product at the water table was based on the idea that LNAPL occurs as a distinct lens in which the drainable pore space is completely saturated with LNAPL. This was often referred to as the "pancake layer" conceptualization (Figure 3). Under the pancake layer paradigm LNAPL saturations are 100 percent. This paradigm predicts large free oil volumes, high mobilities, and large recoverable volumes. Most importantly, the paradigm does not inherently consider soil and product properties as significant. An updated paradigm that is more representative of typical soil capillarity is referred to as the "multiphase" conceptualization, in which LNAPL saturation decreases continuously with depth (Figure 3). In the aquifer, LNAPL coexists in the soil pores with water over a given thickness. An examination of the impacted aquifer indicates that the LNAPL produces a profile with decreasing LNAPL saturation with depth. Specifically, the oil phase will displace the water by pushing into the pore spaces of the upper portions of the profile. With depth, the amount of oil pushing into the pores becomes less and less until at some depth no water is displaced and the pores remain completely filled with water (100 percent water saturation). Field studies have indicated that the multiphase conceptualization provides a good representation for both coarse and fine grained soils.

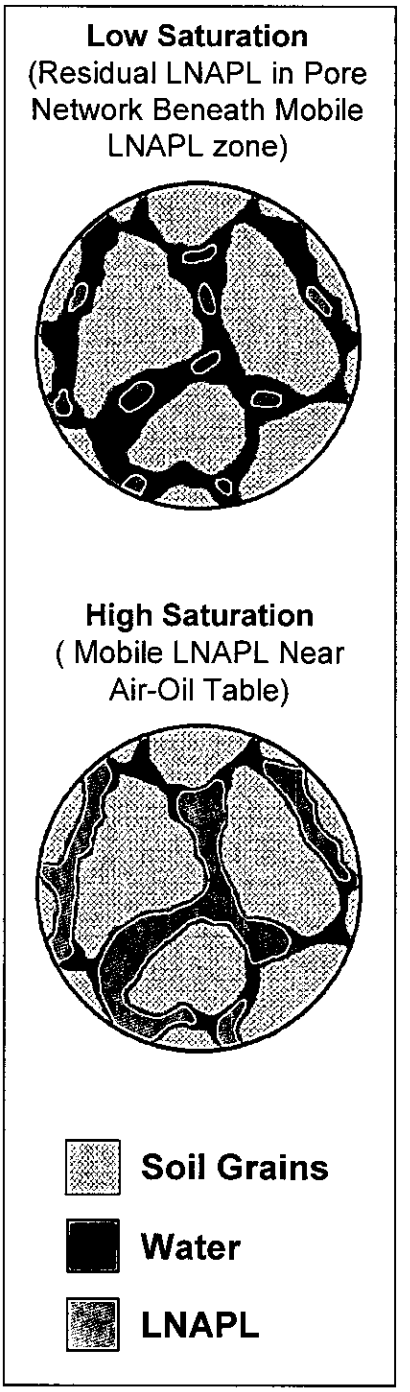

Figure 2. Representation of LNAPL Saturations in the Soil Pore Space.

When a well penetrates LNAPL saturated soil, oil and water will migrate into the well bore and reach equilibrium relative to the atmospheric conditions. As a result, a distinct layer of oil will develop in the well above the water. The thickness of oil in the well will reflect the thickness of the aquifer in which some amount of mobile oil saturation is present (Figure 4). The upper surface of the oil layer in the well is termed the air-oil interface and the lower surface of the oil is termed the oil-water interface. The actual water potentiometric level cannot be physically measured in the well. This interface must be calculated using the density of the oil (ρ_o), the elevation of the water-oil interface (Z_{ow}), and the LNAPL thickness measured in the well (H_o). The following equation is utilized in determining the theoretical air-water interface (Z_{aw}) in a well containing LNAPL.

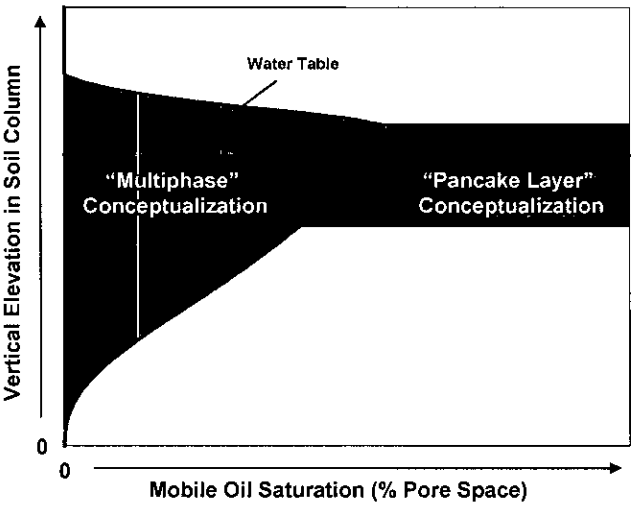

Figure 3. Conceptualization of LNAPL Vertical Distribution in Soil Profile.

$$Z_{aw} = Z_{ow} + (\rho_o H_o) \quad (1)$$

The volume of LNAPL per area of aquifer is primarily dependent upon the properties of the soil and the LNAPL. Since water remains in some of the pore spaces (for some soils, the majority of the pore spaces), the amount of oil in the formation is less than the monitoring well might suggest. In general, for a given observed well product thickness, the mobile LNAPL volume is greater for coarse-grained aquifer material than for soils composed of silt and clay. The importance of grain size is discussed in the primer *Soil Properties*. Similarly, the volume of mobile oil will vary depending on product composition for a given observed well product thickness. The nature and properties of LNAPLs are discussed in the primer *Product Types*.

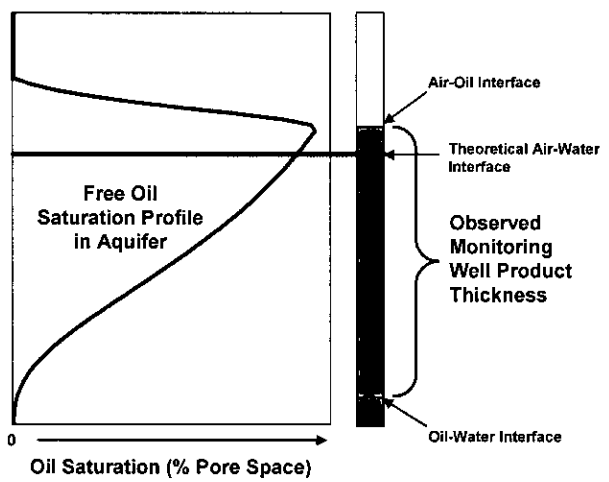

Figure 4. Conceptualization of LNAPL within a Monitoring Well.

Due to capillary forces, some LNAPL is always retained in the soil pores as residual or immobile LNAPL. The remaining "untrapped" LNAPL is mobile and may continue to migrate. As LNAPL moves within the subsurface, the volume of mobile or "free" product continually decreases as LNAPL becomes trapped as isolated droplets within the soil pore network. In particular, it becomes difficult for the oil

to coalesce into a consistent plume of any significant thickness. Hence, LNAPL plumes, unless continually supplied from an on-going release, are "spatially self-limiting." This important concept distinguishes LNAPLs from dissolved and vapor plumes that may migrate significant distances.

Other Considerations

The dynamic and heterogeneous character of the subsurface influences LNAPL conditions. For example, slight differences in soil texture may promote preferential pathways within the aquifer, or conversely, may inhibit product migration causing LNAPL to pool as a stratigraphic trap. Similarly, fractures may create anisotropic conditions that cause product to flow in a direction not directly downgradient. In addition, LNAPL is significantly influenced by vertical fluctuations in the water table. These fluctuations enhance the development of residual LNAPL, which in many cases stabilizes the LNAPL movement. The primers on *Water Table Fluctuations* and *Heterogeneous Conditions* discuss how transient and spatial conditions may influence LNAPL migration.

In the subsurface, constituents composing the LNAPL will begin to transfer from the oil phase to the vapor and liquid phases (Figure 1). The transfer of volatile components to the soil air creates a vapor phase in the unsaturated zone above and adjacent to the LNAPL. Similarly, the transfer of soluble components to the water creates a dissolved plume in the saturated zone. The resulting vapor and dissolved plumes may readily migrate away from the LNAPL plume. In many cases, these plumes contain toxic components that may pose human health and environmental risks. As such, an understanding of the mass transfer between the LNAPL and vapor/water phases is important in managing LNAPL plumes. The concepts of dissolution and volatilization are discussed in the primers *Dissolution* and *Volatilization*.

Because LNAPL may act as a continuing source of dissolved and volatile contamination, numerous technologies have been developed to facilitate recovery of both mobile and residual product. The applicability of the technology depends upon site-specific hydrogeologic conditions, the nature and distribution of the LNAPL, and the remedial objectives. Although remediation techniques are continuing to improve, most technologies remain limited in removing LNAPL from the subsurface. In particular, the extraction of residual LNAPL is problematic and retention of approximately 40 to 70 percent of the LNAPL mass within the aquifer may occur. Furthermore, the application and operation of some technologies may increase the retention of LNAPL. As such, the proper selection and appropriate operation of corrective measures is very important and may significantly influence long-term conditions at a site. These concepts are discussed in greater detail in the primer *Remediation Technologies*.

Since the effectiveness of current remedial efforts for residual phase product is limited, LNAPL contaminated sites need to be managed in a different manner. Perspectives of producing rapid clean-ups to background conditions are impracticable and generally not possible. LNAPL contaminated sites must be understood in terms of risk and managed appropriately. Hence, understanding must be gained in terms of LNAPL plume stability and recoverability as well as a source of contaminant mass transfer to the water and vapor phases. It is from this technical basis that LNAPL risk can be determined.

References

Abdul, A.S., S.F. Kia, and T.L. Gibson. 1989. Limitations of monitoring wells for the detection and qualification of petroleum products in soils and aquifers, *Ground Water Monitoring Report*, Spring 1989: 90-99.

API. 1996. *A Guide to the Assessment and Remediation of Underground Petroleum Releases*, 3rd Edition, Publication Number 1628, American Petroleum Institute, Washington, DC.

Brost, E.J. and G.E. DeVaull. 2000. Non-aqueous phase liquid (NAPL) mobility limits in soil, *Soil and Groundwater Research Bulletin*, No. 9, American Petroleum Institute.

Charbeneau, R.J., R.T. Johns, L.W. Lake, and M.J. McAdams. 1999. *Free-Product Recovery of Petroleum Hydrocarbon Liquids*, Publication Number 4682, American Petroleum Institute, Health and Environmental Sciences Department.

Farr, A.M., R.J. Houghtalen, and D.B. McWhorter. 1990. Volume Estimation of Light Nonaqueous Phase Liquids in Porous Media, *Ground Water*, 28(1): 48-56.

Fetter, C.W. 1993. *Contaminant Hydrogeology*, Macmillan Publishing Company, New York, NY.

Huntley, D. and G.D. Beckett. 2002. *Evaluating Hydrocarbon Removal from Source Zones and its Effect on Dissolved Plume Longevity and Magnitude*, Publication Number 4715, American Petroleum Institute, Regulatory Analysis and Scientific Affairs Department.

Huntley, D., R.N. Hawk, and H.P. Corley. 1994. Nonaqueous phase hydrocarbon in a fine-grained sandstone: 1. comparison between measured and predicted saturations and mobility, *Ground Water*, 32(4): 626-634.

Huntley, D., J.W. Wallace, and R.N. Hawk. 1994. Nonaqueous phase hydrocarbon in a fine-grained sandstone: 2. effect of local sediment variability on the estimation of hydrocarbon volumes, *Ground Water*, 32(5): 778-783.

Kemblowski, M.W. and C.Y. Chiang. 1990. Hydrocarbon thickness fluctuations in monitoring wells, *Ground Water*, 28(2): 244-252.

Lenhard, R.J., T.G. Johnson, and J.C. Parker. 1993. Experimental observations of nonaqueous-phase liquid subsurface movement, *Journal of Contaminant Hydrology*, 12: 79-101, Elsevier Science Publishers B.V., Amsterdam, The Netherlands.

Lenhard, R.J. and J.C. Parker. 1990a. Estimation of free hydrocarbon volume from fluid levels in monitoring wells, *Ground Water*, 28(1): 57-67.

Lenhard, R.J. and J.C. Parker. 1990b. Discussion of estimation of free hydrocarbon volume from fluid levels in monitoring wells, *Ground Water*, 28(5): 800-801.

Lenhard, R.J., T.G. Johnson, and J.C. Parker. 1993. Experimental observations of nonaqueous-phase liquid subsurface movement, *Journal of Contaminant Hydrology*, 12: 79-101, Elsevier Science Publishers B.V., Amsterdam, The Netherlands.

Lundegard, P.D. and B. Mudford. 1995. A modified approach to free product volume estimation, In: *Proceedings of the Petroleum Hydrocarbons and Organic Chemicals in*

Ground Water: Prevention, Detection, and Remediation Conference, Houston, TX, November 29 – December 1, pp. 423-437, Ground Water Publishing Company.

Lundegard, P.D. and B.S. Mudford. 1998. LNAPL volume calculation: Parameter estimation by nonlinear regression of saturation profiles, *Ground Water and Remediation*, 18(3): 88-93.

Lyman, W.J, P.J. Reidy, and B. Levy. 1991. *Assessing UST Corrective Action Technology: A Scientific Evaluation of the Mobility and Degradability of Organic Contaminants in Subsurface Environments*, EPA/600/2-91/053, United States Environmental Protection Agency, Office of Research and Development, Washington, DC.

Mercer, J.W. and R.M. Cohen. 1990. A review of immiscible fluids in the subsurface: Properties, models, characterization, and remediation, *Journal of Contaminant Hydrology*, 6(2): 107-163.

Newell, C.J., S.D. Acree, R.R. Ross, and S.G. Huling. 1995. *Light Non-aqueous Phase Liquids*, EPA-540-5-95-500, United States Environmental Protection Agency, Office of Research and Development, Robert S. Kerr Laboratory, Ada, OK.

Parker, J.C., D.W. Waddill, J.A. Johnson. 1995. *UST Corrective Action Technologies: Engineering Design of Free Product Recovery Systems,* United States Environmental Protection Agency, Risk Reduction Engineering Laboratory Report, Contract No. 68-C2-0108, p.82.

Sale, T. 2001. *Methods for Determining Inputs to Environmental Petroleum Hydrocarbon Mobility and Volume Models*, API Publication 4711, American Petroleum Institute.

U.S. EPA. 1996. *How to Effectively Recover Free Product at Leaking Underground Storage Tank Sites: A Guide for State Regulators*, EPA 510-R-96-001, Office of Solid Waste and Emergency Response, United States Environmental Protection Agency, Washington, DC, and National Risk Management Research Laboratory, United States Environmental Protection Agency, Cincinnati, OH.

APPENDIX B

Appendix B

LNAPL Model Runs

Appendix B.1

MW5 Data Runs

van Genuchten-Burdine Model of LNAPL Distribution and Relative Permeability

Enter Data in Yellow Region

Maximum Monitoring Well LNAPL Thickness [feet]	
b_o =	1.090

Soil Characteristic		
n =	0.380	porosity
N =	2.680	van Genuchten "N"
α =	4.400	van Genuchten "α" [ft^{-1}]
S_{wr} =	0.045	irreducible water saturation
S_{orv} =	0.050	residual LNAPL saturation (vadose)
S_{ors} =	0.150	residual LNAPL saturation (saturated)

Fluid Characteristics:		
ρ_o =	0.900	LNAPL density [gm/cc]
σ_{aw} =	65.000	air/water surface tension [dyne/cm]
σ_{ao} =	25.000	air/LNAPL surface tension [dyne/cm]
σ_{ow} =	25.000	LNAPL/water surface tension [dyne/cm]

Calculated Parameters		
M =	0.627	van Genuchten "M"
α_{ao} =	10.296	air/LNAPL "α" [ft^{-1}]
α_{ow} =	1.144	LNAPL/water "α" [ft^{-1}]
z_{ao} =	0.109	elevation of air-LNAPL interface [ft]
z_{ow} =	-0.981	elevation of LNAPL-water interface [ft]
z_{max} =	0.279	maximum free-product elevation [ft]
λ =	1.124	pore-size distribution index
Ψ_b =	0.148	B-C displacement pressure head [ft]

Set *Tools* > *Option* > *Calculations* tab to "Manual."
Press Ctrl+Shift+S to calculate sheet

b_o [ft]	D_o [ft]	k_{ro}	χ [ft]	β	ξ [ft]	η		
0.000	0.000	0.000						
0.087	0.008	0.000	0.0000	0.087428	0.0000	0.000000		
0.392	0.029	0.000	-0.0213	0.070253	0.0872	0.000472	0.0001	Eps-Do
1.090	0.141	0.044	0.2115	0.160684	0.3901	0.063039	0.00001	Eps-kro

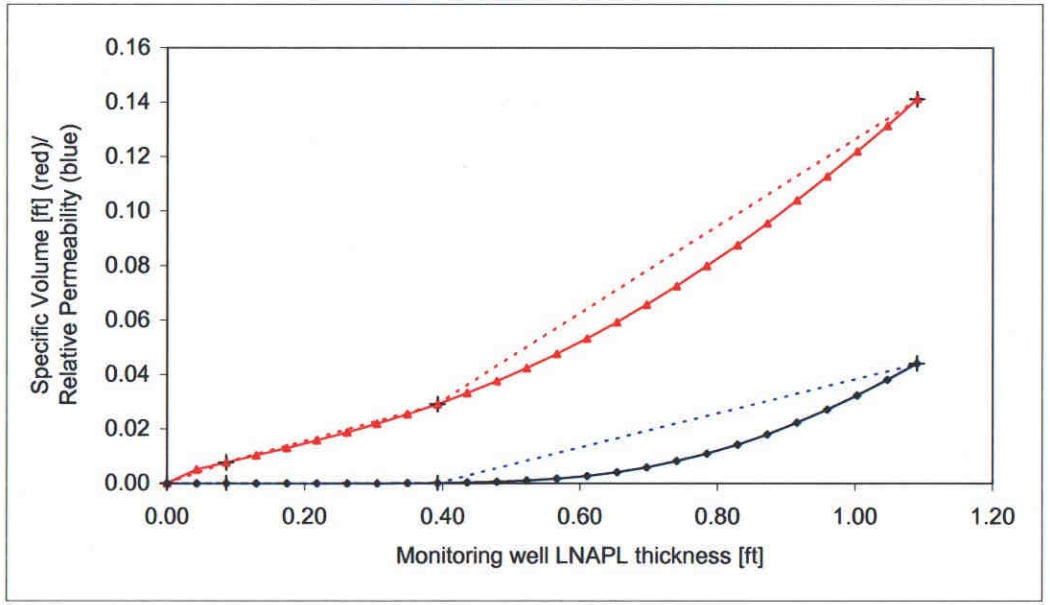

Monitoring Well LNAPL Thickness b_o [ft] =	1.090
D_o [ft] = 0.141	k_{ro} = 0.044

Enter b_o value here to plot corrsponding profiles

Press Ctrl-Shift+S to calculate sheet

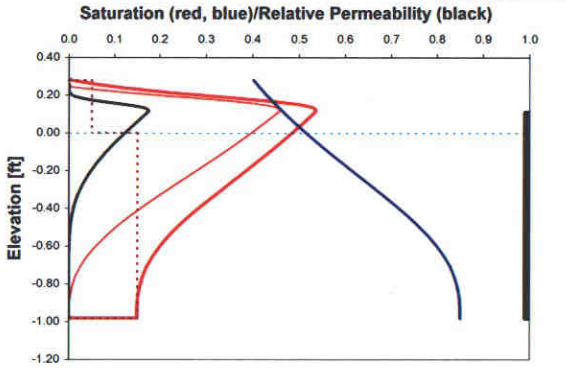

Scale	Elevation	S_o	S_w	Elevation	k_{ro}	so_k		
	0.279	0.000						
0	0.279	0.005	0.402	0.259	0	0	0	0
1	0.273	0.018	0.404	0.254	0	0	1	0
2	0.268	0.031	0.406	0.249	0	0		
3	0.262	0.046	0.408	0.244	5.8206E-08	0.004298701		
4	0.256	0.062	0.410	0.239	8.29175E-06	0.022121656		
5	0.251	0.079	0.412	0.234	5.50951E-05	0.040963661		
6	0.245	0.097	0.414	0.229	0.000189026	0.060833527	z	So
7	0.239	0.116	0.416	0.224	0.000480546	0.08172482	0.279	0
8	0.234	0.136	0.418	0.219	0.001027607	0.10361172	0.279	0.05
9	0.228	0.158	0.420	0.214	0.001961081	0.126444406	0.000	0.05
10	0.222	0.181	0.422	0.209	0.003449014	0.150144114		
11	0.217	0.205	0.424	0.204	0.005698078	0.17459813		
12	0.211	0.231	0.426	0.199	0.008950101	0.199655134	-0.981	0
13	0.205	0.257	0.428	0.194	0.013471133	0.225121479	-0.981	0.15
14	0.200	0.284	0.430	0.189	0.019530643	0.250759124	0.000	0.15
15	0.194	0.311	0.433	0.184	0.027369371	0.276286077	0	0.05
16	0.188	0.339	0.435	0.179	0.037156509	0.301380227		
17	0.183	0.367	0.437	0.174	0.048940284	0.325687306	0.109	0.99
18	0.177	0.394	0.439	0.169	0.062600127	0.348833412	0.109	1
19	0.171	0.420	0.441	0.164	0.077812224	0.370441971	-0.981	1
20	0.166	0.444	0.444	0.159	0.094041513	0.390154322	-0.981	0.99
21	0.160	0.466	0.446	0.154	0.110570346	0.407652341	0.109	0.99
22	0.154	0.485	0.448	0.149	0.126566517	0.422680912		
23	0.149	0.502	0.450	0.144	0.141182709	0.435067772		
24	0.143	0.515	0.453	0.139	0.15366926	0.444738454		
25	0.137	0.525	0.455	0.134	0.163476739	0.451724865		
26	0.132	0.532	0.457	0.129	0.170327071	0.456167205		
27	0.126	0.535	0.459	0.124	0.174241461	0.45831054		
28	0.120	0.536	0.462	0.119	0.175527173	0.458499312		
29	0.115	0.536	0.464	0.114	0.174740542	0.457176795		
30	0.109	0.533	0.467	0.109	0.172672403	0.454913413		
31	0.055	0.510	0.490	0.055	0.147313261	0.427116317		
32	0.000	0.485	0.515	0.000	0.122880171	0.397841222		
33	-0.055	0.460	0.540	-0.055	0.099829803	0.367181563		
34	-0.109	0.433	0.567	-0.109	0.078629483	0.335295223		
35	-0.164	0.405	0.595	-0.164	0.059717465	0.302417306		
36	-0.218	0.377	0.623	-0.218	0.043453135	0.268871063		
37	-0.273	0.348	0.652	-0.273	0.030063822	0.23507445		
38	-0.327	0.320	0.680	-0.327	0.01959963	0.201539209		
39	-0.382	0.292	0.708	-0.382	0.011910615	0.168859204		
40	-0.436	0.266	0.734	-0.436	0.006658852	0.137685375		
41	-0.491	0.242	0.758	-0.491	0.003369491	0.108686471		
42	-0.545	0.220	0.780	-0.545	0.001511313	0.082497536		
43	-0.600	0.200	0.800	-0.600	0.000584267	0.059661532		
44	-0.654	0.184	0.816	-0.654	0.000187108	0.040572297		
45	-0.709	0.171	0.829	-0.709	4.67248E-05	0.025428042		
46	-0.763	0.162	0.838	-0.763	8.22817E-06	0.014202758		
47	-0.818	0.156	0.844	-0.818	8.46103E-07	0.00663827		
48	-0.872	0.152	0.848	-0.872	3.3207E-08	0.002252846		
49	-0.927	0.150	0.850	-0.927	1.27376E-10	0.000352447		
50	-0.981	0.150	0.850	-0.981	0	0		
	-0.981	0.000						

Interfacial and Surface Tension (dynes/cm) at 20° C

(From Charbeneau, et al. 1999. *Free-Product Recovery of Petroleum Hydrocarbon Liquids*. API Publication 4682)

Chemical Name	Interfacial Tension	Surface Tension
Benzene	35	28.9
Ethylbenzene	35.5	29.3
Toluene	36.1	28.5
o-Xylene	36.1	30.3
Crude Oil	no data	24-38
Diesel Fuel	50	25
Gasoline	50	21
Naptha (BTX mixture)	45	20
Fuel Oil No. 1	48	27
Jet Fuel JP-4/5	50	25
Petroleum Distillates	50	21

Source: Mercer, J.W. and Cohen, R. M., A Review of Immiscible Fluids in the Subsurface, *Journal of Contaminant Hydrology*, Vol. 6, pp. 107-163, 1990.

Laboratory measurements show that the values of both the surface and the interfacial tensions of a crude oil extend over a wide range of values, from 2 dyne/cm to 30 dyne/cm. A value of 25 dyne/cm is commonly used for both surface (σ_{ao}) and interfacial (σ_{ow}) tensions of a crude oil. Measurements show that for an unleaded gasoline with 7% MTBE, the interfacial tension is 35.1 dyne/cm (Charbeneau and Chiang, 1995). In the laboratory, the surface tension for water in contact with air is σ_{aw} = 72 dyne/cm. In soil, some chemicals will accumulate at the interface between water and air, reducing the surface tension, and an effective air-water surface tension of 65 dyne/cm is often assumed.

Additional information about interfacial tension values can be found in:

Kolhatker R; Kremesec V, Rubin S, Yukewa C, Senn R. Application Of Field And Analytical Techniques To Evaluate Recoverability Of Subsurface Free Phase Hydrocarbons Proceedings Of The Petroleum Hydrocarbons And Organic Chemicals In Ground Water: Prevention, Detection, And Remediation; Conference And Exposition, November 17-19, 1999, Houston, Texas; p5-15.

LNAPL Parameters Database to be published by API in 2003. (Check www.api.org/lnapl for availability)

Representative LNAPL Density Values (gm/cm^3)

(From Charbeneau, et al. 1999. *Free-Product Recovery of Petroleum Hydrocarbon Liquids*. API Publication 4682)

Fluid Type	Temp.0 °C	Source	Temp.15 °C	Source	Temp.20 °C	Source	Temp.25 °C	Source
Water	1.000	C	0.998	C	0.998	C	0.996	C
Automotive Gasoline	0.746	A	0.729	A				
Automotive Diesel	0.838	A	0.827	A				
Kerosene	0.842	A	0.839	A			0.835	A
Jet Fuel (JP-3)					0.800	B		
Jet Fuel (JP-5)			0.844	A	0.820	B		
Fuel Oil #2	0.874	A	0.868	A	0.840	A		
Fuel Oil #4	0.914	A	0.904	A	0.900	B	0.898	A
Fuel Oil #5	0.932	A	0.923	A			0.917	A
Fuel Oil #6 or Bunker C	0.986	A	0.974	A			0.964	A
Electrical Lubricating Oil	0.882	A	0.974	A				
Electrical Lubricating Oil – used	0.883	A	0.874	A				
Electrical Insulating Oil	0.892	A	0.882	A				
Electrical Insulating Oil – used	0.878	A	0.867	A				
Norman Wells Crude	0.845	A	0.832	A			0.829	A
Avalon Crude	0.848	A	0.839	A			0.834	A
Alberta Crude	0.850	A	0.840	A			0.832	A
Transmoutain Blend Crude	0.865	A	0.855	A				
Bow River Blend Crude	0.900	A	0.893	A			0.885	A
Prudhoe Bay Crude	0.915	A	0.905	A			0.900	A
Atkinson Crude	0.922	A	0.911	A			0.905	A
La Rosa Crude	0.923	A	0.914	A			0.908	A

Source: A-API, 1996; B-Mercer and Cohen, 1990; C-Vennard and Street, 1982

American Petroleum Institute, A Guide to the Assessment and Remediation of Underground Petroleum Releases, API Publication 1628, 3rd Ed., Washington, D.C., July 1996.

Mercer, J.W. and Cohen, R. M., A Review of Immiscible Fluids in the Subsurface, Journal of Contaminant Hydrology, Vol. 6, pp. 107-163, 1990.

Vennard, J. K. and R. L. Street, Elementary Fluid Mechanics (6th Edition), John Wiley and Sons, New York, NY, 1982.

Average Porosity (Standard Deviation) Values Based on Soil Texture

(From Charbeneau, et al. 1999. *Free-Product Recovery of Petroleum Hydrocarbon Liquids*. API Publication 4682)

Soil Type	Porosity (n)
Clay	0.38 (0.09)
Clay Loam	0.41 (0.09)
Loam	0.43 (0.10)
Loamy Sand	0.41 (0.09)
Silt	0.46 (0.11)
Silt Loam	0.45 (0.06)
Silty Clay	0.36 (0.07)
Silty Clay Loam	0.43 (0.07)
Sand	0.43 (0.06)
Sandy Clay	0.38 (0.05)
Sandy Clay Loam	0.39 (0.07)
Sandy Loam	0.41 (0.09)

(Source: Carsell, R. F. and Parish, R. S., Developing Joint Probability Distributions of Soil Water Retention Characteristics, *Water Resources Research*, 24(5), pp. 755-769, 1988.)

LNAPL Residual Saturation and Volumetric Retention Capacity Values (after Mercer and Cohen, 1990).

(From Charbeneau, et al. 1999. *Free-Product Recovery of Petroleum Hydrocarbon Liquids*. API Publication 4682)

Soil Type	R for Gasoline	Gasoline Residual Saturation	R for Middle Distillates	Middle Distillates Residual Saturation	R for Fuel Oil	Fuel Oil Residual Saturation
Coarse Gravel	2.5	0.007	5	0.014	10	0.029
Coarse Sand and Gravel	4	0.011	8	0.023	16	0.046
Medium to Coarse Sand	7.5	0.021	15	0.043	30	0.086
Fine to Medium Sand	12.5	0.036	25	0.071	50	0.143
Silt to Fine Sand	20	0.057	40	0.114	80	0.229
Coarse Sand		0.15 - 0.19				0.12
Medium Sand		0.12 - 0.27		0.19		0.11-0.23
Fine Sand		0.19 - 0.60				
Well Graded Sand		0.46 - 0.59				0.52

Residual LNAPL amounts are reported either in terms of residual saturation or *volumetric retention capacity*, R, defined by:

$$R = S_{or} \times n \times 1000$$

The units for R are liters of residual LNAPL per cubic meter of medium.

Source: Mercer, J.W. and Cohen, R. M., A Review of Immiscible Fluids in the Subsurface, *Journal of Contaminant Hydrology*, Vol. 6, pp. 107-163, 1990.

Additional information about residual saturation values can be found in:

Brost, E.J., Devaull, G.E., *Non-Aqueous Phase Liquid (NAPL) Mobility Limits in Soil*. API Soil and Groundwater Research Bulletin No. 9 June 2000.

Descriptive Statistics from Carsel and Parrish (1988) Data Set Tabulated Values: Mean (Standard Deviation)

(From Charbeneau, et al. 1999. *Free-Product Recovery of Petroleum Hydrocarbon Liquids*. API Publication 4682)

Soil Type	Residual Saturation, S_{or}	Bubbling Pressure Head, Ψ_b (m)*	Pore Size Distribution Index, λ
Clay	0.18 (0.088)	1.25 (1.88)	0.09 (0.09)
Clay loam	0.23 (0.024)	0.53 (0.42)	0.31 (0.09)
Loam	0.18 (0.030)	0.28 (0.16)	0.56 (0.11)
Loamy sand	0.14 (0.037)	0.081 (0.028)	1.28 (0.27)
Silt	0.074 (0.022)	0.62 (0.27)	0.37 (0.05)
Silty loam	0.15 (0.033)	0.50 (0.30)	0.41 (0.12)
Silty clay	0.19 (0.064)	2.0 (2.0)	0.09 (0.06)
Silty clay loam	0.21 (0.021)	1.0 (0.6)	0.23 (0.06)
Sand	0.10 (0.023)	0.069 (0.014)	1.68 (0.29)
Sandy clay	0.26 (0.034)	0.37 (0.23)	0.23 (0.19)
Sandy clay loam	0.26 (0.015)	0.17 (0.11)	0.48 (0.13)
Sandy loam	0.16 (0.041)	0.13 (0.066)	0.89 (0.17)

*Carsel and Parrish (1988) report mean and standard deviation of van Genuchten's 'α' parameter. The standard deviation of Ψ_b is approximated by:

$$\sigma_{\Psi_b} \cong \frac{\sigma_{\frac{1}{\alpha}}}{\alpha^2}.$$

(Source: Carsell, R. F. and Parish, R. S., Developing Joint Probability Distributions of Soil Water Retention Characteristics, *Water Resources Research*, 24(5), pp. 755-769, 1988.)

REPRESENTATIVE VAN GENUCHTEN MODEL PARAMETERS (AFTER CARSELL AND PARISH, 1988)

Soil type	Sample Size	Saturated Water Content, θ_m		Residual Water Content, θ_{wr}		van Genuchten N		van Genuchten α (ft^{-1})		Hydraulic Conductivity K_{ws} (ft/d)		
		mean	std. dev.	mean	std. dev.	mean	std. dev.	mean	std. dev.	sample size	mean	std. dev.
Clay	400	0.38	0.09	0.068	0.034	1.09	0.09	0.24	0.37	114	0.16	0.33
Clay Loam	364	0.41	0.09	0.095	0.010	1.31	0.09	0.58	0.46	345	0.20	0.56
Loam	735	0.43	0.10	0.078	0.013	1.56	0.11	1.1	0.64	735	0.82	1.44
Loamy Sand	315	0.41	0.09	0.057	0.015	2.28	0.27	3.8	1.3	315	11	8.9
Silt	82	0.46	0.11	0.034	0.010	1.37	0.05	0.49	0.21	88	0.20	0.26
Silt Loam	1093	0.45	0.08	0.067	0.015	1.41	0.12	0.61	0.37	1093	0.36	0.98
Silty Clay	374	0.36	0.07	0.070	0.023	1.09	0.06	0.15	0.15	126	0.016	0.085
Silty Clay Loam	641	0.43	0.07	0.089	0.009	1.23	0.06	0.30	0.18	592	0.056	0.15
Sand	246	0.43	0.06	0.045	0.010	2.68	0.29	4.4	0.88	246	23	12
Sandy Clay	46	0.38	0.05	0.100	0.013	1.23	0.10	0.82	0.52	46	0.095	0.22
Sandy Clay Loam	214	0.39	0.07	0.100	0.006	1.48	0.13	1.8	1.2	214	1.0	2.2
Sandy Loam	1183	0.41	0.09	0.065	0.017	1.89	0.17	2.3	1.1	1183	3.6	4.6

(Source: Carsell, R. F. and Parish, R. S., Developing Joint Probability Distributions of Soil Water Retention Characteristics, *Water Resources Research*, 24(5), pp. 755-769, 1988.)

0.8	1.2	0.048	0.1
1.9	1.5	0.062	0.17
3.6	2.1	0.25	0.44
12.4	4.3	3.5	2.7
1.6	0.7	0.06	0.079
2	1.2	0.11	0.3
0.5	0.5	0.0048	0.026
1	0.6	0.017	0.046
14.5	2.9	7.1	3.7
2.7	1.7	0.029	0.067
5.9	3.8	0.31	0.66
7.5	3.7	1.1	1.4

MW5 Water Enhanced Recovery

Free-Product Recovery System Analysis

$t_{recovery}$ [yr] =	5
R_c [ft] =	30
μ_o [cp] =	378
K_w [ft/d] =	32
r_{well} [ft] =	0.33

Water Enhanced

Q_w [gpm] =	5
b_{well} [ft] =	1
$R_{influence}$ [ft] =	50
s_{well} [ft] =	24.04

Vacuum Enhanced

(-) p_w [atm]	0
L_{well} [ft] =	10
$\underline{k}_{ra}$ =	0.9
Q_{air} [scfm] =	0.0
h_{well} [ft H_2O] =	0.0

Skimmer Well

If Q_w = 0 and p_w = 0 then a skimmer well is assumed

Average drawdown (buildup) within radius of capture

s_w [ft] = 4.84

Press Ctrl-Shift+S to calculate sheet

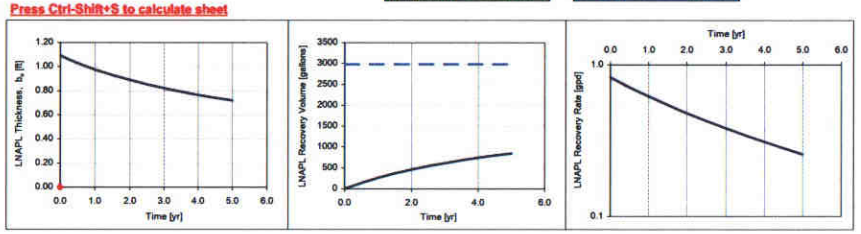

γ =	0.053200
A_w^* [d^{-1}] =	8.11E-04
A_a^* [d^{-1}] =	0.00E+00
A_o^* [$ft^{-1}d^{-1}$] =	1.88E-06
t_2 [yr] =	69.4874
t_1 [yr] =	14470.4855

Index	Time [yr]	Time [d]	$b_o(t)$ [ft]	$V_o(t)$ [gallon]	$Q_o(t)$ [gpd]
0	0.00	0	1.090	0.00	0.82
1	0.00	0	1.090	0.00	0.82
2	0.00	0	1.090	0.00	0.82
3	0.00	0	1.090	0.00	0.82
4	0.00	0	1.090	0.00	0.82
5	0.00	0	1.090	0.00	0.82
6	0.00	0	1.090	0.00	0.82
7	0.00	0	1.090	0.00	0.82
8	0.00	0	1.090	0.00	0.82
9	0.00	0	1.090	0.00	0.82
10	0.00	0	1.090	0.00	0.82
11	0.50	183	1.029	139.60	0.71
12	1.00	365	0.975	260.38	0.62
13	1.50	548	0.929	365.84	0.54
14	2.00	730	0.888	458.67	0.48
15	2.50	913	0.852	540.97	0.43
16	3.00	1095	0.820	614.39	0.38
17	3.50	1278	0.791	680.27	0.34
18	4.00	1460	0.765	739.67	0.31
19	4.50	1643	0.741	793.48	0.28
20	5.00	1825	0.719	842.42	0.26
21	5.00	1825	0.719	842.42	0.26
22	5.00	1825	0.719	842.42	0.26
23	5.00	1825	0.719	842.42	0.26
24	5.00	1825	0.719	842.42	0.26
25	5.00	1825	0.719	842.42	0.26
26	5.00	1825	0.719	842.42	0.26
27	5.00	1825	0.719	842.42	0.26
28	5.00	1825	0.719	842.42	0.26
29	5.00	1825	0.719	842.42	0.26
30	5.00	1825	0.719	842.42	0.26
31	5.00	1825	0.719	842.42	0.26
32	5.00	1825	0.719	842.42	0.26
33	5.00	1825	0.719	842.42	0.26
34	5.00	1825	0.719	842.42	0.26
35	5.00	1825	0.719	842.42	0.26
36	5.00	1825	0.719	842.42	0.26
37	5.00	1825	0.719	842.42	0.26
38	5.00	1825	0.719	842.42	0.26
39	5.00	1825	0.719	842.42	0.26
40	5.00	1825	0.719	842.42	0.26

t	bo
0.0000	0
0.0000	0

t	vo
0	2985.374
5	2985.374

MW5 Vacuum Enhanced Recovery

Free-Product Recovery System Analysis

$t_{recovery}$ [yr] =	5
R_c [ft] =	30
μ_o [cp] =	378
K_w [ft/d] =	32
r_{well} [ft] =	0.33

Water Enhanced	
Q_w [gpm] =	5
b_{well} [ft] =	1
$R_{influence}$ [ft] =	50
s_{well} [ft] =	24.04

Vacuum Enhanced	
(-) p_w [atm]	1
L_{well} [ft] =	10
h_{cs} =	0.9
Q_{air} [scfm] =	524.6
h_{well} [ft H_2O] =	-33.9

Skimmer Well

If Q_w = 0 and p_w = 0 then a skimmer well is assumed

Average drawdown (buildup) within radius of capture

s_w [ft] = 1.08

Press Ctrl-Shift+S to calculate sheet

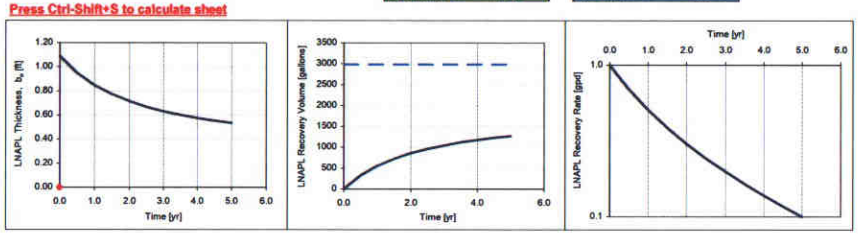

γ =	0.053200
A_w^* [d^{-1}] =	8.11E-04
A_o^* [d^{-1}] =	1.27E-03
A_s^* [$ft^{-1}d^{-1}$] =	1.88E-06
t_2 [yr] =	27.0414
t_1 [yr] =	5631.2693

Index	Time [yr]	Time [d]	$b_o(t)$ [ft]	$V_o(t)$ [gallon]	$Q_o(t)$ [gpd]
0	0.00	0	1.090	0.00	1.00
1	0.00	0	1.090	0.00	1.00
2	0.00	0	1.090	0.00	1.00
3	0.00	0	1.090	0.00	1.00
4	0.00	0	1.090	0.00	1.00
5	0.00	0	1.090	0.00	1.00
6	0.00	0	1.090	0.00	1.00
7	0.00	0	1.090	0.00	1.00
8	0.00	0	1.090	0.00	1.00
9	0.00	0	1.090	0.00	1.00
10	0.00	0	1.090	0.00	1.00
11	0.50	183	0.948	322.14	0.69
12	1.00	365	0.847	551.70	0.51
13	1.50	548	0.772	723.00	0.39
14	2.00	730	0.714	855.28	0.30
15	2.50	913	0.668	960.15	0.24
16	3.00	1095	0.630	1045.05	0.20
17	3.50	1278	0.600	1114.93	0.16
18	4.00	1460	0.574	1173.26	0.14
19	4.50	1643	0.552	1222.51	0.12
20	5.00	1825	0.534	1264.51	0.10
21	5.00	1825	0.534	1264.51	0.10
22	5.00	1825	0.534	1264.51	0.10
23	5.00	1825	0.534	1264.51	0.10
24	5.00	1825	0.534	1264.51	0.10
25	5.00	1825	0.534	1264.51	0.10
26	5.00	1825	0.534	1264.51	0.10
27	5.00	1825	0.534	1264.51	0.10
28	5.00	1825	0.534	1264.51	0.10
29	5.00	1825	0.534	1264.51	0.10
30	5.00	1825	0.534	1264.51	0.10
31	5.00	1825	0.534	1264.51	0.10
32	5.00	1825	0.534	1264.51	0.10
33	5.00	1825	0.534	1264.51	0.10
34	5.00	1825	0.534	1264.51	0.10
35	5.00	1825	0.534	1264.51	0.10
36	5.00	1825	0.534	1264.51	0.10
37	5.00	1825	0.534	1264.51	0.10
38	5.00	1825	0.534	1264.51	0.10
39	5.00	1825	0.534	1264.51	0.10
40	5.00	1825	0.534	1264.51	0.10

t	bo
0.0000	0
0.0000	0

t	vo
0	2985.374
5	2985.374

MW5 Reduced Viscosity (Heat)

Free-Product Recovery System Analysis

$t_{recovery}$ [yr] =	5
R_o [ft] =	30
μ_o [cp] =	101
K_w [ft/d] =	32
r_{well} [ft] =	0.33

Water Enhanced

Q_w [gpm] =	5
b_{well} [ft] =	1
$R_{influence}$ [ft] =	50
s_{well} [ft] =	24.04

Vacuum Enhanced

(-) p_w [atm]	0
L_{well} [ft] =	10
$\underline{k}_{rs}$ =	0.9
Q_{air} [scfm] =	0.0
h_{well} [ft H_2O] =	0.0

Skimmer Well

If Q_w = 0 and p_w = 0 then a skimmer well is assumed

Average drawdown (buildup) within radius of capture

s_r [ft] =	4.84

Press Ctrl-Shift+S to calculate sheet

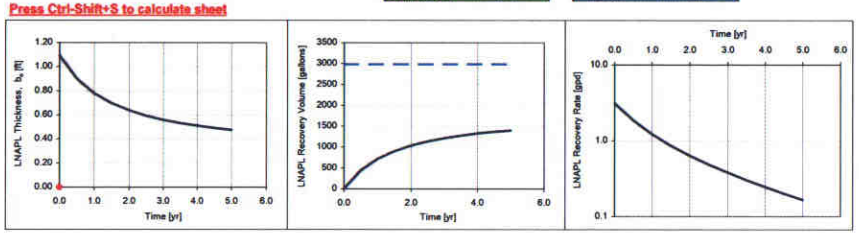

γ =	0.053200
A_w^* [d^{-1}] =	3.03E-03
A_a^* [d^{-1}] =	0.00E+00
A_s^* [$ft^{-1}d^{-1}$] =	7.03E-06
t_2 [yr] =	18.5667
t_1 [yr] =	3866.4525

Index	Time [yr]	Time [d]	$b_o(t)$ [ft]	$V_o(t)$ [gallon]	$Q_o(t)$ [gpd]
0	0.00	0	1.090	0.00	3.09
1	0.00	0	1.090	0.00	3.09
2	0.00	0	1.090	0.00	3.09
3	0.00	0	1.090	0.00	3.09
4	0.00	0	1.090	0.00	3.09
5	0.00	0	1.090	0.00	3.09
6	0.00	0	1.090	0.00	3.09
7	0.00	0	1.090	0.00	3.09
8	0.00	0	1.090	0.00	3.09
9	0.00	0	1.090	0.00	3.09
10	0.00	0	1.090	0.00	3.09
11	0.50	183	0.898	435.85	1.85
12	1.00	365	0.778	709.84	1.22
13	1.50	548	0.696	896.74	0.86
14	2.00	730	0.636	1031.45	0.63
15	2.50	913	0.592	1132.44	0.48
16	3.00	1095	0.558	1210.41	0.38
17	3.50	1278	0.530	1271.97	0.30
18	4.00	1460	0.509	1321.46	0.24
19	4.50	1643	0.491	1361.81	0.20
20	5.00	1825	0.476	1395.10	0.17
21	5.00	1825	0.476	1395.10	0.17
22	5.00	1825	0.476	1395.10	0.17
23	5.00	1825	0.476	1395.10	0.17
24	5.00	1825	0.476	1395.10	0.17
25	5.00	1825	0.476	1395.10	0.17
26	5.00	1825	0.476	1395.10	0.17
27	5.00	1825	0.476	1395.10	0.17
28	5.00	1825	0.476	1395.10	0.17
29	5.00	1825	0.476	1395.10	0.17
30	5.00	1825	0.476	1395.10	0.17
31	5.00	1825	0.476	1395.10	0.17
32	5.00	1825	0.476	1395.10	0.17
33	5.00	1825	0.476	1395.10	0.17
34	5.00	1825	0.476	1395.10	0.17
35	5.00	1825	0.476	1395.10	0.17
36	5.00	1825	0.476	1395.10	0.17
37	5.00	1825	0.476	1395.10	0.17
38	5.00	1825	0.476	1395.10	0.17
39	5.00	1825	0.476	1395.10	0.17
40	5.00	1825	0.476	1395.10	0.17

t	bo
0.0000	0
0.0000	0

t	vo
0	2985.374
5	2985.374

MW5 Trench Recovery

Trench Recovery System

Press Ctrl+Shift+S to calculate sheet

$t_{recovery}$ [yr] =	5
μ_o [cp] =	378
Q_w [gpm] =	10
J_w =	0.007
K_w [ft/d] =	32
W_T [ft] =	150
L_T [ft] =	200
b_T [ft] =	1.09

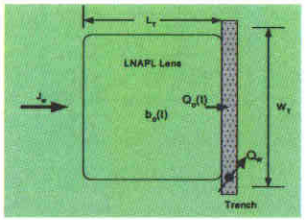

Recoverable Volume

0	31675.80
5	31675.80

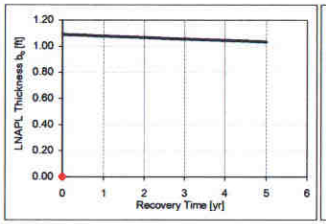

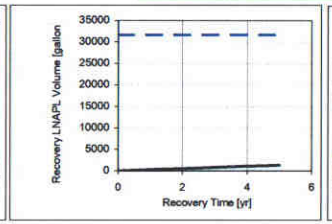

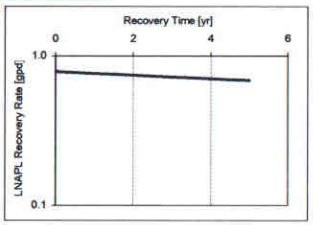

t	bo
0.00	0
0.00	0

γ =	0.05320
A_T [d^{-1}] =	7.28E-05
t_2 [yr] =	774.18
t_1 [yr] =	161220.7

Index	Time [yr]	Time [d]	$b_o(t)$ [ft]	$V_o(t)$ [gallon]	$Q_o(t)$ [gpd]
0	0.000	0	1.090	0.00	0.79
1	0.000	0	1.090	0.00	0.79
2	0.000	0	1.090	0.00	0.79
3	0.000	0	1.090	0.00	0.79
4	0.000	0	1.090	0.00	0.79
5	0.000	0	1.090	0.00	0.79
6	0.000	0	1.090	0.00	0.79
7	0.000	0	1.090	0.00	0.79
8	0.000	0	1.090	0.00	0.79
9	0.000	0	1.090	0.00	0.79
10	0.000	0	1.090	0.00	0.79
11	0.500	183	1.084	142.29	0.77
12	1.000	365	1.078	282.63	0.76
13	1.500	548	1.073	421.05	0.75
14	2.000	730	1.067	557.59	0.74
15	2.500	913	1.061	692.28	0.73
16	3.000	1095	1.056	825.18	0.72
17	3.500	1278	1.050	956.30	0.71
18	4.000	1460	1.045	1085.69	0.70
19	4.500	1643	1.040	1213.38	0.70
20	5.000	1825	1.034	1339.39	0.69
21	5.000	1825	1.034	1339.39	0.69
22	5.000	1825	1.034	1339.39	0.69
23	5.000	1825	1.034	1339.39	0.69
24	5.000	1825	1.034	1339.39	0.69
25	5.000	1825	1.034	1339.39	0.69
26	5.000	1825	1.034	1339.39	0.69
27	5.000	1825	1.034	1339.39	0.69
28	5.000	1825	1.034	1339.39	0.69
29	5.000	1825	1.034	1339.39	0.69
30	5.000	1825	1.034	1339.39	0.69
31	5.000	1825	1.034	1339.39	0.69
32	5.000	1825	1.034	1339.39	0.69
33	5.000	1825	1.034	1339.39	0.69
34	5.000	1825	1.034	1339.39	0.69
35	5.000	1825	1.034	1339.39	0.69
36	5.000	1825	1.034	1339.39	0.69
37	5.000	1825	1.034	1339.39	0.69
38	5.000	1825	1.034	1339.39	0.69
39	5.000	1825	1.034	1339.39	0.69
40	5.000	1825	1.034	1339.39	0.69

Appendix B.2

MW13 Data Runs

van Genuchten-Burdine Model of LNAPL Distribution and Relative Permeability

Enter Data in Yellow Region

Maximum Monitoring Well LNAPL Thickness [feet]	
b_o =	0.490

Soil Characteristic		
n =	0.380	porosity
N =	2.680	van Genuchten "N"
α =	4.400	van Genuchten "α" [ft^{-1}]
S_{wr} =	0.045	irreducible water saturation
S_{orv} =	0.050	residual LNAPL saturation (vadose)
S_{ors} =	0.150	residual LNAPL saturation (saturated)

Fluid Characteristics:		
ρ_o =	0.900	LNAPL density [gm/cc]
σ_{aw} =	65.000	air/water surface tension [dyne/cm]
σ_{ao} =	25.000	air/LNAPL surface tension [dyne/cm]
σ_{ow} =	25.000	LNAPL/water surface tension [dyne/cm]

Calculated Parameters		
M =	0.627	van Genuchten "M"
α_{ao} =	10.296	air/LNAPL "α" [ft^{-1}]
α_{ow} =	1.144	LNAPL/water "α" [ft^{-1}]
z_{ao} =	0.049	elevation of air-LNAPL interface [ft]
z_{ow} =	-0.441	elevation of LNAPL-water interface [ft]
z_{max} =	0.139	maximum free-product elevation [ft]
λ =	1.124	pore-size distribution index
Ψ_b =	0.148	B-C displacement pressure head [ft]

Set *Tools* > *Option* > *Calculations* tab to "Manual."
Press Ctrl+Shift+S to calculate sheet

b_o [ft]	D_o [ft]	k_{ro}	χ [ft]	β	ξ [ft]	η		
0.000	0.000	0.000						
0.039	0.005	0.000	0.0000	0.123278	0.0000	0.000000		
0.176	0.013	0.000	-0.0416	0.059794	0.0392	0.000002	0.0001	Eps-Do
0.490	0.039	0.001	0.0167	0.081606	0.1763	0.002167	0.00001	Eps-kro

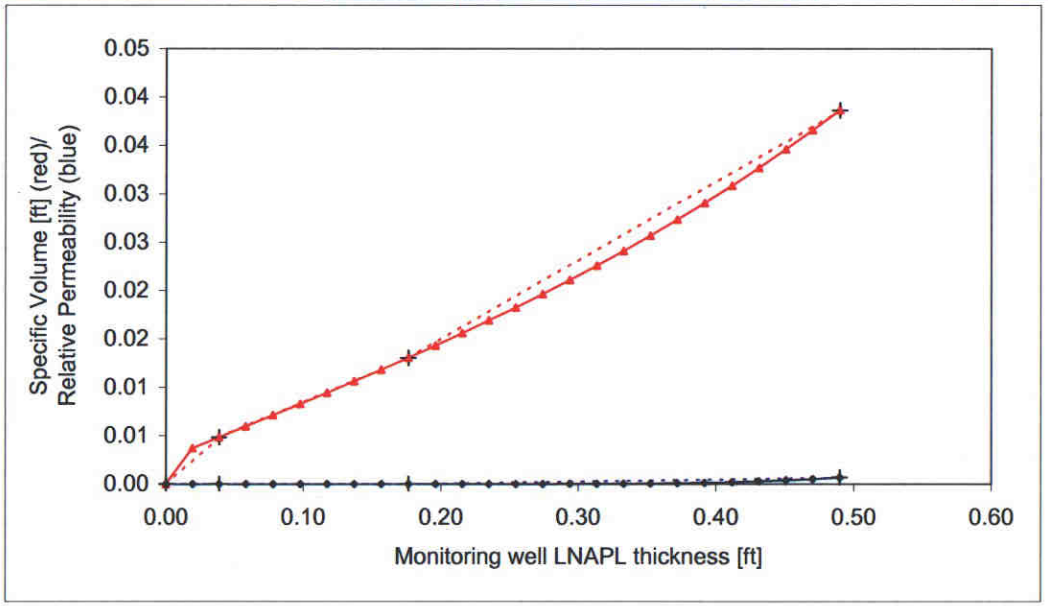

Monitoring Well LNAPL Thickness b_o [ft] =			0.490
D_o [ft] =	0.039	k_{ro} =	0.001

Enter b_o value here to plot corrsponding profiles

Press Ctrl-Shift+S to calculate sheet

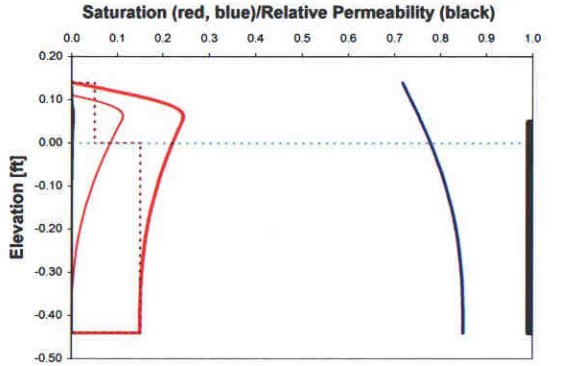

Scale	Elevation	S_o	S_w	Elevation	k_{ro}	so_k
	0.139	0.000				
0	0.139	0.001	0.717	0.129	0	0
1	0.136	0.015	0.719	0.126	0	0
2	0.133	0.029	0.720	0.124	0	0
3	0.130	0.044	0.722	0.121	0	0
4	0.127	0.058	0.723	0.118	0	0
5	0.124	0.072	0.724	0.116	0	0
6	0.121	0.087	0.726	0.113	0	0
7	0.118	0.101	0.727	0.110	0	0
8	0.115	0.114	0.729	0.108	3.24823E-06	0.01134641
9	0.112	0.128	0.730	0.105	2.60954E-05	0.022608441
10	0.109	0.141	0.732	0.102	8.5071E-05	0.033359021
11	0.106	0.153	0.733	0.100	0.000191904	0.043546562
12	0.103	0.165	0.734	0.097	0.000353047	0.05312338
13	0.100	0.176	0.736	0.094	0.000569568	0.062046679
14	0.097	0.186	0.737	0.092	0.00083741	0.070279472
15	0.094	0.196	0.739	0.089	0.001148024	0.077791428
16	0.091	0.205	0.740	0.086	0.001489303	0.084559596
17	0.088	0.213	0.741	0.084	0.001846738	0.090569003
18	0.085	0.220	0.743	0.081	0.002204694	0.095813092
19	0.082	0.226	0.744	0.078	0.002547689	0.100294004
20	0.079	0.231	0.745	0.076	0.002861559	0.104022704
21	0.076	0.235	0.747	0.073	0.003134429	0.107018951
22	0.073	0.239	0.748	0.070	0.00335741	0.109311154
23	0.070	0.241	0.749	0.068	0.003525006	0.110936133
24	0.067	0.243	0.751	0.065	0.003635216	0.111938847
25	0.064	0.244	0.752	0.062	0.003689371	0.112372145
26	0.061	0.245	0.753	0.060	0.003691774	0.112296662
27	0.058	0.244	0.755	0.057	0.003649199	0.111781027
28	0.055	0.244	0.756	0.054	0.003570375	0.110902724
29	0.052	0.243	0.757	0.052	0.003465574	0.109750531
30	0.049	0.241	0.759	0.049	0.003346752	0.108432515
31	0.025	0.231	0.769	0.025	0.002371278	0.096288747
32	0.000	0.221	0.779	0.000	0.001635972	0.084767814
33	-0.025	0.212	0.788	-0.025	0.0010961	0.073917444
34	-0.049	0.204	0.796	-0.049	0.00071099	0.063779424
35	-0.074	0.196	0.804	-0.074	0.00044487	0.054388626
36	-0.098	0.189	0.811	-0.098	0.000267342	0.045772156
37	-0.123	0.182	0.818	-0.123	0.000153486	0.037948642
38	-0.147	0.176	0.824	-0.147	8.36376E-05	0.030927695
39	-0.172	0.171	0.829	-0.172	4.29039E-05	0.024709545
40	-0.196	0.166	0.834	-0.196	2.05005E-05	0.019284862
41	-0.221	0.162	0.838	-0.221	8.99839E-06	0.014634743
42	-0.245	0.159	0.841	-0.245	3.5604E-06	0.010730851
43	-0.270	0.156	0.844	-0.270	1.23668E-06	0.007535659
44	-0.294	0.154	0.846	-0.294	3.62702E-07	0.005002757
45	-0.319	0.153	0.847	-0.319	8.45547E-08	0.003077126
46	-0.343	0.151	0.849	-0.343	1.41577E-08	0.00169529
47	-0.368	0.151	0.849	-0.368	1.40756E-09	0.000785138
48	-0.392	0.150	0.850	-0.392	5.41784E-11	0.000265051
49	-0.417	0.150	0.850	-0.417	2.06078E-13	4.13714E-05
50	-0.441	0.150	0.850	-0.441	0	0
	-0.441	0.000				

z	So
0.139	0
0.139	0.05
0.000	0.05
-0.441	0
-0.441	0.15
0.000	0.15
0	0.05
0.049	0.99
0.049	1
-0.441	1
-0.441	0.99
0.049	0.99

Interfacial and Surface Tension (dynes/cm) at 20° C

(From Charbeneau, et al. 1999. *Free Product Recovery of Petroleum Hydrocarbon Liquids*. API Publication 4682)

Chemical Name	Interfacial Tension	Surface Tension
Benzene	35	28.9
Ethylbenzene	35.5	29.3
Toluene	36.1	28.5
o-Xylene	36.1	30.3
Crude Oil	no data	24-38
Diesel Fuel	50	25
Gasoline	50	21
Naptha (BTX mixture)	45	20
Fuel Oil No. 1	48	27
Jet Fuel JP-4/5	50	25
Petroleum Distillates	50	21

Source: Mercer, J.W. and Cohen, R. M., A Review of Immiscible Fluids in the Subsurface, *Journal of Contaminant Hydrology*, Vol. 6, pp. 107-163, 1990.

Laboratory measurements show that the values of both the surface and the interfacial tensions of a crude oil extend over a wide range of values, from 2 dyne/cm to 30 dyne/cm. A value of 25 dyne/cm is commonly used for both surface (σ_{ao}) and interfacial (σ_{ow}) tensions of a crude oil. Measurements show that for an unleaded gasoline with 7% MTBE, the interfacial tension is 35.1 dyne/cm (Charbeneau and Chiang, 1995). In the laboratory, the surface tension for water in contact with air is σ_{aw} = 72 dyne/cm. In soil, some chemicals will accumulate at the interface between water and air, reducing the surface tension, and an effective air-water surface tension of 65 dyne/cm is often assumed.

Additional information about interfacial tension values can be found in:

Kolhatker R; Kremesec V, Rubin S, Yukawa C, Senn R. Application Of Field And Analytical Techniques To Evaluate Recoverability Of Subsurface Free Phase Hydrocarbons Proceedings Of The Petroleum Hydrocarbons And Organic Chemicals In Ground Water: Prevention, Detection, And Remediation; Conference And Exposition, November 17-19, 1999, Houston, Texas; p5-15.

LNAPL Parameters Database to be published by API in 2003. (Check www.api.org/lnapl for availability)

Representative LNAPL Density Values (gm/cm^3)

(From Charbeneau, et al. 1999. *Free Product Recovery of Petroleum Hydrocarbon Liquids*. API Publication 4682)

Fluid Type	Temp.0 °C	Source	Temp.15 °C	Source	Temp.20 °C	Source	Temp.25 °C	Source
Water	1.000	C	0.998	C	0.998	C	0.996	C
Automotive Gasoline	0.746	A	0.729	A				
Automotive Diesel	0.838	A	0.827	A				
Kerosene	0.842	A	0.839	A			0.835	A
Jet Fuel (JP-3)					0.800	B		
Jet Fuel (JP-5)			0.844	A	0.820	B		
Fuel Oil #2	0.874	A	0.866	A	0.840	A		
Fuel Oil #4	0.914	A	0.904	A	0.900	B	0.898	A
Fuel Oil #5	0.932	A	0.923	A			0.917	A
Fuel Oil #6 or Bunker C	0.986	A	0.974	A			0.964	A
Electrical Lubricating Oil	0.882	A	0.974	A				
Electrical Lubricating Oil – used	0.883	A	0.874	A				
Electrical Insulating Oil	0.892	A	0.882	A				
Electrical Insulating Oil – used	0.878	A	0.867	A				
Norman Wells Crude	0.845	A	0.832	A			0.829	A
Avalon Crude	0.846	A	0.839	A			0.834	A
Alberta Crude	0.850	A	0.840	A			0.832	A
Transmoutain Blend Crude	0.865	A	0.855	A				
Bow River Blend Crude	0.900	A	0.893	A			0.885	A
Prudhoe Bay Crude	0.915	A	0.905	A			0.900	A
Atkinson Crude	0.922	A	0.911	A			0.905	A
La Rosa Crude	0.923	A	0.914	A			0.908	A

Source: A-API, 1996; B-Mercer and Cohen, 1990; C-Vennard and Street, 1982

American Petroleum Institute, A Guide to the Assessment and Remediation of Underground Petroleum Releases, API Publication 1628, 3rd Ed., Washington, D.C., July 1996.

Mercer, J.W. and Cohen, R. M., A Review of Immiscible Fluids in the Subsurface, Journal of Contaminant Hydrology, Vol. 6, pp. 107-163, 1990.

Vennard, J. K. and R. L. Street, Elementary Fluid Mechanics (6th Edition), John Wiley and Sons, New York, NY, 1982.

Average Porosity (Standard Deviation) Values Based on Soil Texture

(From Charbeneau, et al. 1999. *Free-Product Recovery of Petroleum Hydrocarbon Liquids*. API Publication 4682)

Soil Type	Porosity (n)
Clay	0.38 (0.09)
Clay Loam	0.41 (0.09)
Loam	0.43 (0.10)
Loamy Sand	0.41 (0.09)
Silt	0.46 (0.11)
Silt Loam	0.45 (0.08)
Silty Clay	0.36 (0.07)
Silty Clay Loam	0.43 (0.07)
Sand	0.43 (0.06)
Sandy Clay	0.38 (0.05)
Sandy Clay Loam	0.39 (0.07)
Sandy Loam	0.41 (0.09)

(Source: Carsell, R. F. and Parish, R. S., Developing Joint Probability Distributions of Soil Water Retention Characteristics, *Water Resources Research*, 24(5), pp. 755-769, 1988.)

LNAPL Residual Saturation and Volumetric Retention Capacity Values (after Mercer and Cohen, 1990).

(From Charbeneau, et al. 1999. *Free-Product Recovery of Petroleum Hydrocarbon Liquids*. API Publication 4682)

Soil Type	R for Gasoline	Gasoline Residual Saturation	R for Middle Distillates	Middle Distillates Residual Saturation	R for Fuel Oil	Fuel Oil Residual Saturation
Coarse Gravel	2.5	0.007	5	0.014	10	0.029
Coarse Sand and Gravel	4	0.011	8	0.023	16	0.046
Medium to Coarse Sand	7.5	0.021	15	0.043	30	0.086
Fine to Medium Sand	12.5	0.036	25	0.071	50	0.143
Silt to Fine Sand	20	0.057	40	0.114	80	0.229
Coarse Sand		0.15 - 0.19				0.12
Medium Sand		0.12 - 0.27		0.19		0.11-0.23
Fine Sand		0.19 - 0.60				
Well Graded Sand		0.46 - 0.59				0.52

Residual LNAPL amounts are reported either in terms of residual saturation or *volumetric retention capacity*, R, defined by:

$$R = S_{or} \times n \times 1000$$

The units for R are liters of residual LNAPL per cubic meter of medium.

Source: Mercer, J.W. and Cohen, R. M., A Review of Immiscible Fluids in the Subsurface, *Journal of Contaminant Hydrology*, Vol. 6, pp. 107-163, 1990.

Additional information about residual saturation values can be found in:

Brost, E.J., Devaull, G.E., *Non-Aqueous Phase Liquid (NAPL) Mobility Limits in Soil*. API Soil and Groundwater Research Bulletin No. 9 June 2000.

Descriptive Statistics from Carsel and Parrish (1988) Data Set Tabulated Values: Mean (Standard Deviation)

(From Charbeneau, et al. 1999. *Free-Product Recovery of Petroleum Hydrocarbon Liquids*. API Publication 4682)

Soil Type	Residual Saturation, S_{or}	Bubbling Pressure Head, Ψ_b (m)*	Pore Size Distribution Index, λ
Clay	0.18 (0.069)	1.25 (1.88)	0.09 (0.09)
Clay loam	0.23 (0.024)	0.53 (0.42)	0.31 (0.09)
Loam	0.18 (0.030)	0.28 (0.15)	0.56 (0.11)
Loamy sand	0.14 (0.037)	0.081 (0.026)	1.28 (0.27)
Silt	0.074 (0.022)	0.82 (0.27)	0.37 (0.05)
Silty loam	0.15 (0.033)	0.50 (0.30)	0.41 (0.12)
Silty clay	0.19 (0.064)	2.0 (2.0)	0.09 (0.06)
Silty clay loam	0.21 (0.021)	1.0 (0.6)	0.23 (0.06)
Sand	0.10 (0.023)	0.069 (0.014)	1.68 (0.29)
Sandy clay	0.26 (0.034)	0.37 (0.23)	0.23 (0.19)
Sandy clay loam	0.26 (0.015)	0.17 (0.11)	0.48 (0.13)
Sandy loam	0.16 (0.041)	0.13 (0.066)	0.89 (0.17)

*Carsel and Parrish (1988) report mean and standard deviation of van Genuchten's 'α' parameter. The standard deviation of Ψ_b is approximated by:

$$\sigma_{\Psi_b} \approx \frac{\sigma_{\alpha}}{\alpha^2}.$$

(Source: Carsell, R. F. and Parish, R. S., Developing Joint Probability Distributions of Soil Water Retention Characteristics, *Water Resources Research*, 24(5), pp. 755-769, 1988.)

REPRESENTATIVE VAN GENUCHTEN MODEL PARAMETERS (AFTER CARSELL AND PARISH, 1988)

Soil type	Sample Size	Saturated Water Content, θ_m		Residual Water Content, θ_{wr}		van Genuchten N		van Genuchten α (ft^{-1})		Hydraulic Conductivity K_{ws} (ft/d)		
		mean	std. dev.	mean	std. dev.	mean	std. dev.	mean	std. dev.	sample size	mean	std. dev.
Clay	400	0.38	0.09	0.068	0.034	1.09	0.09	0.24	0.37	114	0.16	0.33
Clay Loam	364	0.41	0.09	0.095	0.010	1.31	0.09	0.58	0.46	345	0.20	0.56
Loam	735	0.43	0.10	0.078	0.013	1.56	0.11	1.1	0.64	735	0.82	1.44
Loamy Sand	315	0.41	0.09	0.057	0.015	2.28	0.27	3.8	1.3	315	11	8.9
Silt	82	0.46	0.11	0.034	0.010	1.37	0.05	0.49	0.21	88	0.20	0.26
Silt Loam	1093	0.45	0.08	0.067	0.015	1.41	0.12	0.61	0.37	1093	0.36	0.98
Silty Clay	374	0.36	0.07	0.070	0.023	1.09	0.06	0.15	0.15	126	0.016	0.085
Silty Clay Loam	641	0.43	0.07	0.089	0.009	1.23	0.06	0.30	0.18	592	0.056	0.15
Sand	246	0.43	0.06	0.045	0.010	2.68	0.29	4.4	0.88	246	23	12
Sandy Clay	46	0.38	0.05	0.100	0.013	1.23	0.10	0.82	0.52	46	0.095	0.22
Sandy Clay Loam	214	0.39	0.07	0.100	0.006	1.48	0.13	1.8	1.2	214	1.0	2.2
Sandy Loam	1183	0.41	0.09	0.065	0.017	1.89	0.17	2.3	1.1	1183	3.6	4.6

(Source: Carsell, R. F. and Parish, R. S., Developing Joint Probability Distributions of Soil Water Retention Characteristics, *Water Resources Research*, 24(5), pp. 755-769, 1988.)

0.8	1.2
1.9	1.5
3.6	2.1
12.4	4.3
1.6	0.7
2	1.2
0.5	0.5
1	0.6
14.5	2.9
2.7	1.7
5.9	3.8
7.5	3.7

0.048	0.1
0.062	0.17
0.25	0.44
3.5	2.7
0.06	0.079
0.11	0.3
0.0048	0.026
0.017	0.046
7.1	3.7
0.029	0.067
0.31	0.66
1.1	1.4

MW13 Water Enhanced Recovery

Free-Product Recovery System Analysis

$t_{recovery}$ [yr] =	5
R_c [ft] =	30
μ_o [cp] =	21.2
K_w [ft/d] =	32
r_{well} [ft] =	0.33

Water Enhanced	
Q_w [gpm] =	5
b_{well} [ft] =	1
$R_{influence}$ [ft] =	40
s_{well} [ft] =	22.97

Vacuum Enhanced	
(-) p_w [atm]	0
L_{well} [ft] =	10
k_{ra} =	0.9
Q_{air} [scfm] =	0.0
h_{well} [ft H_2O] =	0.0

Skimmer Well

If Q_w = 0 and p_w = 0 then a skimmer well is assumed

Average drawdown (buildup) within radius of capture

s_c [ft] = 3.77

Press Ctrl-Shift+S to calculate sheet

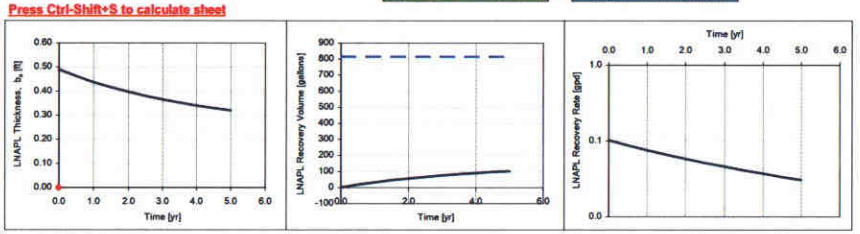

t	bo
0.0000	0
0.0000	0

t	vo
0	816.9497
5	816.9497

γ =	0.053200
A_w^* [d^{-1}] =	1.45E-02
A_o^* [d^{-1}] =	0.00E+00
A_s^* [$ft^{-1}d^{-1}$] =	3.35E-05
t_2 [yr] =	94.1260
t_1 [yr] =	149829.6083

Index	Time [yr]	Time [d]	$b_o(t)$ [ft]	$V_o(t)$ [gallon]	$Q_o(t)$ [gpd]
0	0.00	0	0.490	0.00	0.10
1	0.00	0	0.490	0.00	0.10
2	0.00	0	0.490	0.00	0.10
3	0.00	0	0.490	0.00	0.10
4	0.00	0	0.490	0.00	0.10
5	0.00	0	0.490	0.00	0.10
6	0.00	0	0.490	0.00	0.10
7	0.00	0	0.490	0.00	0.10
8	0.00	0	0.490	0.00	0.10
9	0.00	0	0.490	0.00	0.10
10	0.00	0	0.490	0.00	0.10
11	0.50	183	0.461	17.19	0.09
12	1.00	365	0.437	31.99	0.08
13	1.50	548	0.415	44.84	0.07
14	2.00	730	0.397	56.10	0.06
15	2.50	913	0.380	66.05	0.05
16	3.00	1095	0.365	74.89	0.05
17	3.50	1278	0.352	82.80	0.04
18	4.00	1460	0.340	89.91	0.04
19	4.50	1643	0.330	96.34	0.03
20	5.00	1825	0.320	102.17	0.03
21	5.00	1825	0.320	102.17	0.03
22	5.00	1825	0.320	102.17	0.03
23	5.00	1825	0.320	102.17	0.03
24	5.00	1825	0.320	102.17	0.03
25	5.00	1825	0.320	102.17	0.03
26	5.00	1825	0.320	102.17	0.03
27	5.00	1825	0.320	102.17	0.03
28	5.00	1825	0.320	102.17	0.03
29	5.00	1825	0.320	102.17	0.03
30	5.00	1825	0.320	102.17	0.03
31	5.00	1825	0.320	102.17	0.03
32	5.00	1825	0.320	102.17	0.03
33	5.00	1825	0.320	102.17	0.03
34	5.00	1825	0.320	102.17	0.03
35	5.00	1825	0.320	102.17	0.03
36	5.00	1825	0.320	102.17	0.03
37	5.00	1825	0.320	102.17	0.03
38	5.00	1825	0.320	102.17	0.03
39	5.00	1825	0.320	102.17	0.03
40	5.00	1825	0.320	102.17	0.03

MW13 Vacuum Enhanced Recovery

Free-Product Recovery System Analysis

$t_{recovery}$ [yr] =	5
R_E [ft] =	30
μ_o [cp] =	21.2
K_w [ft/d] =	32
r_{well} [ft] =	0.33

Water Enhanced	
Q_w [gpm] =	5
b_{well} [ft] =	1
$R_{influence}$ [ft] =	40
s_{well} [ft] =	22.97

Vacuum Enhanced	
(-) p_w [atm]	1
L_{well} [ft] =	10
β_{ra} =	0.9
Q_{air} [scfm] =	524.6
h_{well} [ft H_2O] =	-33.9

Skimmer Well

If Q_w = 0 and p_w = 0 then a skimmer well is assumed

Average drawdown (buildup) within radius of capture

s_{ro} [ft] = 0.02

Press Ctrl-Shift+S to calculate sheet

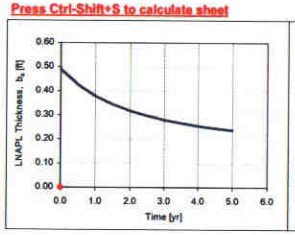

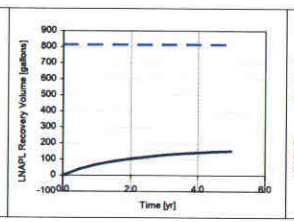

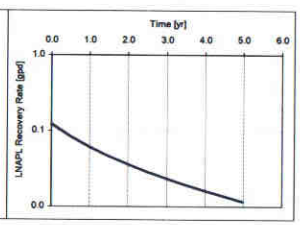

t	bo
0.0000	0
0.0000	0

t	vo
0	816.9497
5	816.9497

γ =	0.053200
A_w^* [d^{-1}] =	1.45E-02
A_a^* [d^{-1}] =	2.27E-02
A_s^* [$ft^{-1}d^{-1}$] =	3.35E-05
t_2 [yr] =	36.6297
t_1 [yr] =	58307.0193

Index	Time [yr]	Time [d]	$b_o(t)$ [ft]	$V_o(t)$ [gallon]	$Q_o(t)$ [gpd]
0	0.00	0	0.490	0.00	0.12
1	0.00	0	0.490	0.00	0.12
2	0.00	0	0.490	0.00	0.12
3	0.00	0	0.490	0.00	0.12
4	0.00	0	0.490	0.00	0.12
5	0.00	0	0.490	0.00	0.12
6	0.00	0	0.490	0.00	0.12
7	0.00	0	0.490	0.00	0.12
8	0.00	0	0.490	0.00	0.12
9	0.00	0	0.490	0.00	0.12
10	0.00	0	0.490	0.00	0.12
11	0.50	183	0.424	39.52	0.08
12	1.00	365	0.378	67.34	0.06
13	1.50	548	0.344	87.92	0.05
14	2.00	730	0.317	103.70	0.04
15	2.50	913	0.297	116.13	0.03
16	3.00	1095	0.280	126.14	0.02
17	3.50	1278	0.266	134.35	0.02
18	4.00	1460	0.255	141.18	0.02
19	4.50	1643	0.245	146.91	0.01
20	5.00	1825	0.237	151.79	0.01
21	5.00	1825	0.237	151.79	0.01
22	5.00	1825	0.237	151.79	0.01
23	5.00	1825	0.237	151.79	0.01
24	5.00	1825	0.237	151.79	0.01
25	5.00	1825	0.237	151.79	0.01
26	5.00	1825	0.237	151.79	0.01
27	5.00	1825	0.237	151.79	0.01
28	5.00	1825	0.237	151.79	0.01
29	5.00	1825	0.237	151.79	0.01
30	5.00	1825	0.237	151.79	0.01
31	5.00	1825	0.237	151.79	0.01
32	5.00	1825	0.237	151.79	0.01
33	5.00	1825	0.237	151.79	0.01
34	5.00	1825	0.237	151.79	0.01
35	5.00	1825	0.237	151.79	0.01
36	5.00	1825	0.237	151.79	0.01
37	5.00	1825	0.237	151.79	0.01
38	5.00	1825	0.237	151.79	0.01
39	5.00	1825	0.237	151.79	0.01
40	5.00	1825	0.237	151.79	0.01

MW13 Reduced Viscosity (Heat)

Free-Product Recovery System Analysis

$t_{recovery}$ [yr] =	5
R_c [ft] =	30
μ_o [cp] =	9.8
K_w [ft/d] =	32
r_{well} [ft] =	0.33

Water Enhanced	
Q_w [gpm] =	5
b_{well} [ft] =	1
$R_{influence}$ [ft] =	40
s_{well} [ft] =	22.97

Vacuum Enhanced	
(-) p_w [atm]	0
L_{well} [ft] =	10
k_{ra} =	0.9
Q_{air} [scfm] =	0.0
h_{well} [ft H_2O] =	0.0

Skimmer Well

If Q_w = 0 and p_w = 0 then a skimmer well is assumed

Average drawdown (buildup) within radius of capture	
s_c [ft] =	3.77

Press Ctrl-Shift+S to calculate sheet

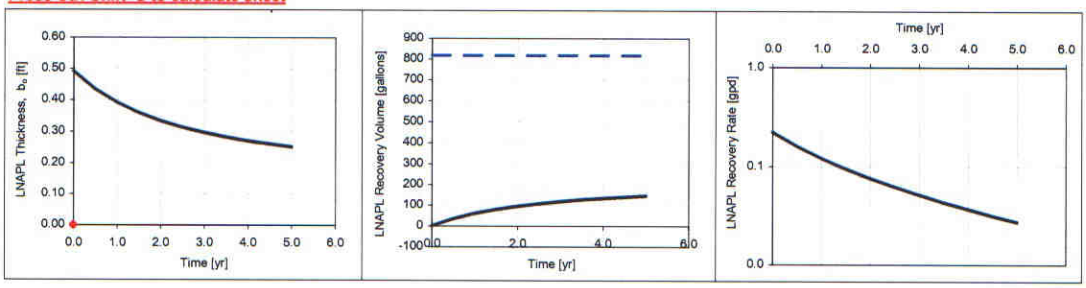

t	bo
0.0000	0
0.0000	0

t	vo
0	816.9497
5	816.9497

γ =	0.053200
A_w^* [d^{-1}] =	3.13E-02
A_a^* [d^{-1}] =	0.00E+00
A_s^* [$ft^{-1}d^{-1}$] =	7.24E-05
t_2 [yr] =	43.5111
t_1 [yr] =	69260.8567

Index	Time [yr]	Time [d]	$b_o(t)$ [ft]	$V_o(t)$ [gallon]	$Q_o(t)$ [gpd]
0	0.00	0	0.490	0.00	0.22
1	0.00	0	0.490	0.00	0.22
2	0.00	0	0.490	0.00	0.22
3	0.00	0	0.490	0.00	0.22
4	0.00	0	0.490	0.00	0.22
5	0.00	0	0.490	0.00	0.22
6	0.00	0	0.490	0.00	0.22
7	0.00	0	0.490	0.00	0.22
8	0.00	0	0.490	0.00	0.22
9	0.00	0	0.490	0.00	0.22
10	0.00	0	0.490	0.00	0.22
11	0.50	183	0.433	34.21	0.16
12	1.00	365	0.391	59.48	0.12
13	1.50	548	0.359	78.88	0.09
14	2.00	730	0.333	94.18	0.07
15	2.50	913	0.313	106.54	0.06
16	3.00	1095	0.296	116.69	0.05
17	3.50	1278	0.282	125.17	0.04
18	4.00	1460	0.270	132.32	0.04
19	4.50	1643	0.260	138.43	0.03
20	5.00	1825	0.251	143.69	0.03
21	5.00	1825	0.251	143.69	0.03
22	5.00	1825	0.251	143.69	0.03
23	5.00	1825	0.251	143.69	0.03
24	5.00	1825	0.251	143.69	0.03
25	5.00	1825	0.251	143.69	0.03
26	5.00	1825	0.251	143.69	0.03
27	5.00	1825	0.251	143.69	0.03
28	5.00	1825	0.251	143.69	0.03
29	5.00	1825	0.251	143.69	0.03
30	5.00	1825	0.251	143.69	0.03
31	5.00	1825	0.251	143.69	0.03
32	5.00	1825	0.251	143.69	0.03
33	5.00	1825	0.251	143.69	0.03
34	5.00	1825	0.251	143.69	0.03
35	5.00	1825	0.251	143.69	0.03
36	5.00	1825	0.251	143.69	0.03
37	5.00	1825	0.251	143.69	0.03
38	5.00	1825	0.251	143.69	0.03
39	5.00	1825	0.251	143.69	0.03
40	5.00	1825	0.251	143.69	0.03

APPENDIX C

Appendix C

Huntley Article
(Persistence of LNAPL sources: Relationship between risk reduction and LNAPL recovery)

ELSEVIER

Journal of Contaminant Hydrology 59 (2002) 3–26

JOURNAL OF
Contaminant
Hydrology

www.elsevier.com/locate/jconhyd

Persistence of LNAPL sources: relationship between risk reduction and LNAPL recovery

David Huntley[a,*], G.D. Beckett[b]

[a] *Department of Geological Sciences, San Diego State University, San Diego, CA 92107, USA*
[b] *AQUI-VER Inc., 6830 La Jolla Blvd., #205, La Jolla, CA 92037, USA*

Received 10 April 2001; received in revised form 18 January 2002; accepted 19 January 2002

Abstract

Light nonaqueous phase liquids (LNAPLs), such as fuels, are the source of much soil and groundwater contamination. Though the mobility of LNAPLs is limited in many environments, dissolved-phase components, such as benzene, can produce groundwater plumes that are more mobile than the LNAPL source. In such a setting, it is commonly assumed that recovery of the LNAPL will result in a reduction in risk associated with the dissolved phase. This paper synthesizes several existing multiphase and chemical transport solutions into a single linked methodology that predicts concentrations of soluble constituents within and downgradient of LNAPL source zones from dissolution of those constituents into groundwater flowing through and below LNAPL sources. This approach has been applied to a variety of LNAPL spill conditions. For biodegradable compounds, these analyses show that the period of time where the dissolved-phase plume is expanding is very small compared to the duration of most LNAPL sources, and that the downgradient extent is generally less than about 100 m for BTEX compounds. Therefore, the risk to receptors, as measured by the maximum downgradient extent of dissolved-phase plume or the maximum concentration of these compounds at a downgradient receptor, is generally unrelated to the longevity of the LNAPL sources. The maximum downgradient extent of the dissolved-phase plume is determined almost entirely by the groundwater velocity and the biodegradation rate. These analyses further demonstrate that recovery of LNAPL by hydraulic methods is often ineffective at reducing risk. Except in coarse-grained soils or intermediate soils with significant LNAPL saturations, free-product recovery approaches do not result in significant reductions in the longevity of downgradient dissolved-phase contamination. Further, for biodegradable constituents, remediation does not result in a near-term decrease in the downgradient extent of contamination. Cleanup methods that act to change the composition of

* Corresponding author. Tel.: +1-619-594-5483; fax: +1-619-594-4372.
E-mail address: david.huntley@geology.sdsu.edu (D. Huntley).

0169-7722/02/$ - see front matter
PII: S0169-7722(02)00073-6

the LNAPL source are more effective at reducing the downgradient concentrations, particularly for fine-grained soils or when LNAPL saturations are low.

Keywords: LNAPL; Dissolution; Biodegradation; Remediation; Risk

1. Introduction

The release of light nonaqueous phase liquids (LNAPLs), such as petroleum fuels, to the subsurface is common throughout the world, ranging in size from small leaks from tanks and pipes to multimillion gallon releases from refining and production operations. Where the volume of the leak is sufficient to reach the water table, the LNAPL poses three separate risks to the environment: (1) direct discharge of LNAPLs to receptors, such as rivers, wells, and springs; (2) vapor phase discharge of volatile constituents to the receptors, such as buildings, subsurface structures, and utility trenches; (3) dissolved-phase constituents in groundwater. Accordingly, most U.S. regulatory agencies require LNAPL recovery at sites exhibiting free product in monitoring wells "to the extent practicable". Clearly, where LNAPL saturations (percent of pore space occupied by LNAPL) are high enough that LNAPL is sufficiently mobile to present a risk of discharge to receptors, remediation resulting in a reduction of LNAPL mass and saturation is necessary to reduce risk. Where this is not the case, however, most regulatory agencies have worked under the assumption that mass removal will result in a reduction in dissolved-phase contaminant concentration and a significant reduction in source longevity. While understandable, the effectiveness of liquid phase recovery in decreasing concentrations (or risk) is often undefined because of the complexity of multiphase flow as well as the complex distribution of NAPL in a heterogeneous system. The relation between remediation, concentration change, and risk is of fundamental importance to effectively manage resources and bring about the environmental protections we seek.

Though the mobility of LNAPLs is limited in many environments, dissolved-phase components, such as benzene, are widely recognized to produce groundwater plumes that are more mobile than the LNAPL source. Research over the past several years, however, has suggested that natural biodegradation of many of these dissolved-phase components can limit potential health and resource impacts. A simplified release and degradation scenario has four phases.

(1) Release of the LNAPL and downward movement through the vadose zone. In many cases, the volume of LNAPL released is small and may result only in a vadose zone impact. The resulting risk to potential receptors in this case is limited to vapor phase impacts and potential leaching of dissolved-phase constituents to the groundwater table, although biodegradation reactions often limit a leachate impact.

(2) If the volume of release is sufficient, the LNAPL will ultimately arrive at the water table and result in the growth of a dissolved-phase plume (Fig. 1). The LNAPL distributes itself in the capillary fringe and aquifer according to the weight of the product mass (i.e., head) and the soil and fluid properties. Because the product does not fully displace the

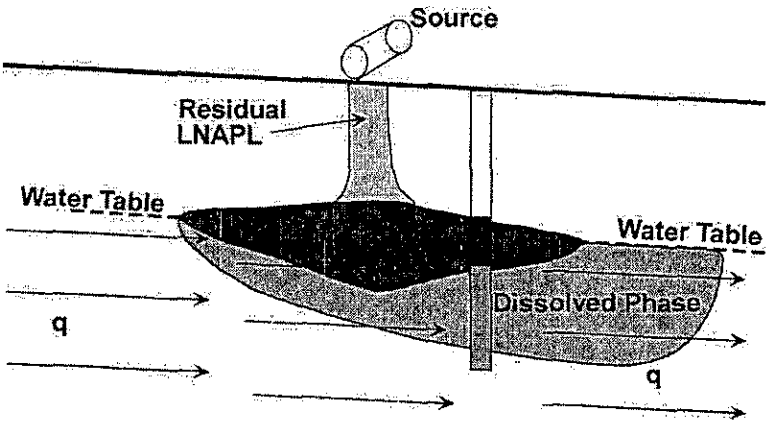

Fig. 1. Conceptual model of LNAPL source dissolution.

water in pores, dissolved-phase mass is contributed from both within and below the product pool.

(3) For biodegradable constituents, a pseudo-steady-state occurs where mass removal of dissolved-phase components by biodegradation keeps pace with the rate of dissolution from the LNAPL source. If the constituent of concern is less degradable, such as MTBE, the plume will expand to a greater degree and dilution will play a greater role in attenuation. This will typically result in a larger plume than one limited by biodegradation.

(4) Eventually, the dissolved-phase plume contracts as the LNAPL source is depleted. This happens most rapidly for LNAPL pools of small mass and length.

Increasingly, regulators are being asked to close sites based on arguments of minimal risk, supported in large part by research that shows that biodegradation limits the growth of dissolved-phase plumes. Many of these same regulators express discomfort with closing sites with significant free-product hydrocarbon (LNAPL), particularly because most sites observed today exhibit a stable, non-contracting dissolved-phase plume. For instance, of 271 sites evaluated in California, 59% of the plumes were stable, 8% were expanding and 33% contracting (Rice et al., 1995), despite the fact that half the sites studied had free-product thicknesses of less than 0.1 ft. Further, regulations may simply require LNAPL cleanup to the degree practical (e.g., California Health and Safety Code, Title 23, Section 26550).

The purpose of this paper is to provide a method to assess (1) how long LNAPL provides a source of dissolved-phase contaminants of concern in the aquifer; (2) the expected time period of expanding, steady-state, and contracting dissolved-phase plumes; (3) how risk is related to the duration (or persistence) of an LNAPL source; and (4) the degree to which risk and dissolved-phase concentrations are reduced by such hydraulic free-product recovery. The focus is on the dissolution and volatilization of a dissolved-phase constituent, such as benzene, from an LNAPL source that is observable in monitoring wells as free-product floating on groundwater.

This same general approach linking the LNAPL distribution and mass to dissolution and transport in groundwater applies equally to residual-phase LNAPL trapped below the groundwater table. For the purposes of comparison, this paper assumes LNAPL saturation

distributions produced by vertical equilibrium. It does not does not incorporate, for example, the effects of vertical redistribution of LNAPL produced by a fluctuating water table (smearing). Ultimately, however, the real-world distribution of the LNAPL in the aquifer determines both the mass and the rate of mass loss by dissolution in any system. Sites characterized by thin zones of LNAPL observed in wells where there is no "smear zone" will behave much differently than sites characterized by the same observed thickness, but with a significant mass of LNAPL smeared below that interval. The authors are preparing a follow-up paper that discusses complexities observed at a variety of field sites exhibiting different LNAPL conditions. The reader is cautioned to accept the theoretical comparisons that follow only within their underlying assumptions.

It should be noted that the approach described in these papers does not incorporate biodegradation of hydrocarbon within the source itself, only in the dissolved-phase downgradient of the source area. This process is omitted because the importance of biodegradation in source areas and controls on rates are considered uncertain by some. In particular, though it is clear that biodegradation is limited by the flux of electron acceptors, such as oxygen and sulfate, into the source area, it is unclear how that flux would be partitioned amongst the various constituents of concern.

2. Theoretical background

The depletion of an LNAPL source by dissolution will be a function of the original mass of the soluble constituent of concern (such as benzene), the solubility (or effective solubility) of that constituent of concern, and the distribution of specific discharge (q) of groundwater both below and within the LNAPL source. Specifically, the mass rate of depletion of the soluble constituent of concern at any instant in time is given by the product of the specific discharge and the concentration (C) of the soluble constituent, or qC, integrated vertically through and below the LNAPL interval and laterally across the width of the plume. The length of time that an LNAPL contributes dissolved-phase constituents to groundwater is a function of that rate of depletion and the original mass of the soluble constituent, or $V_n\rho_n f_m$, where V_n is the volume of the LNAPL, ρ_n is the density of the LNAPL, and f_m is the mass fraction of soluble constituent m of the LNAPL.

Similarly, the depletion of an LNAPL by volatilization will be a function of the original mass of the constituent of concern, the vapor pressure of that constituent, the vapor diffusion coefficient, the distance to and concentration at a surface boundary, and the surface area of the LNAPL.

2.1. NAPL distribution and volume

The theoretical work of Lenhard and Parker (1990) and Farr et al. (1990), supported by the field observations (Huntley et al., 1994; Lundegard and Mudford, 1998), effectively demonstrates that, under vertical equilibrium conditions, LNAPL and water coexist in the soil pore space between the LNAPL/water and LNAPL/air interfaces measured in adjacent wells. LNAPL saturation (the percentage of the pore space occupied by LNAPL) at the LNAPL/water interface is zero, increasing upward and peaking somewhat above the

LNAPL/air interface. Because LNAPL occupies only a portion of the pore space in the formation between the two interfaces, there is a volume exaggeration of LNAPL in the well. The soil capillary properties can be combined with the measured thickness of LNAPL in the monitoring well to calculate the distribution of LNAPL in the formation. This is based on the extension of soil capillarity equations (Van Genuchten, 1980) from simple air/water systems to LNAPL/water and LNAPL/air systems. This extension allows us to calculate the water saturation (S_w) as a function of the height above the LNAPL/water interface:

$$S_w = (1 - S_r)\left[1 + \left(\alpha_{ow}\frac{P_c^{ow}}{\gamma_w}\right)^n\right]^{-(1-1/n)} + S_r \quad (1)$$

where S_r is the residual saturation, P_c^{ow}/γ_w is the LNAPL/water (oil/water) capillary pressure head, given by:

$$\frac{P_c^{ow}}{\gamma_w} = (1 - \rho_r)h_{ow} \quad (2)$$

α_{ow} and n are the Van Genuchten parameters that describe the shape of the soil moisture retention curve, h_{ow} is the height above the LNAPL/water interface, and ρ_r is the relative density of the LNAPL (Fig. 2). Though α_{ow} can be inferred directly from capillary measurements in the oil/water system, it is more often scaled from the air/water system through the ratio of interfacial tensions($\alpha_{ow} = \alpha_{aw}\sigma_{nw}/\sigma_{ow}$), where α_{aw} is the Van Genuchten fitting constant for an air/water system, and $\sigma_{aw,ow}$ are the air/water and oil/water interfacial tensions. Below the LNAPL/air interface, the total fluid saturation, which is

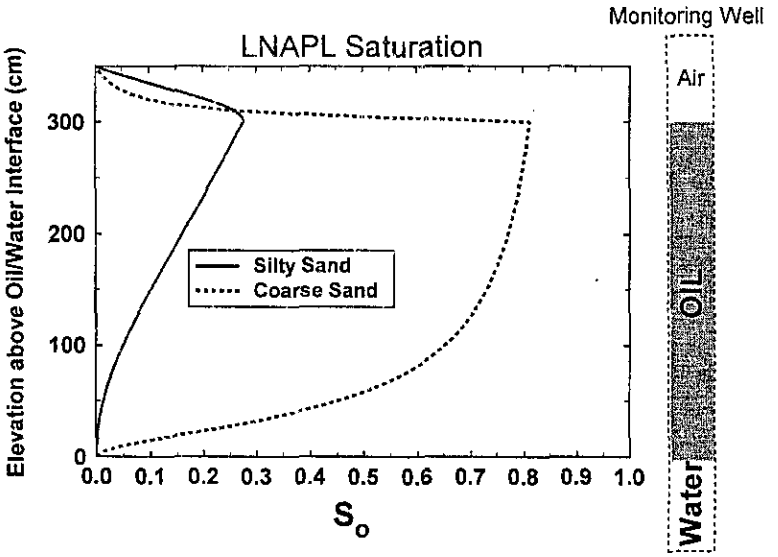

Fig. 2. LNAPL saturation profile for coarse- and fine-grained soils with 3 m of LNAPL in a monitoring well.

simply the sum of the water saturation (S_w) and the LNAPL saturation (S_o), is 1. Above the LNAPL/air interface, the total fluid saturation can be calculated by:

$$S_o + S_w = (1 - S_r)\left[1 + \left(\alpha_{ao}\frac{P_c^{ao}}{\gamma_w}\right)^n\right]^{-\left(1-\frac{1}{n}\right)} + S_r \tag{3}$$

where P_c^{ao}/γ_w is the LNAPL/air (oil/air) capillary pressure head, given by:

$$\frac{P_c^{oa}}{\gamma_w} = \rho_r h_{oa} \tag{4}$$

where α_{oa} is the oil/air Van Genuchten parameter, and h_{oa} is the height above the LNAPL/air interface. The resulting LNAPL saturation profile is the result of subtracting the water saturation from the total fluid ($S_w + S_o$) as a function of height above the LNAPL/water interface (Fig. 2). The total volume (V_o) is simply:

$$V_o = \varphi \int_0^{surf} S_o dz \tag{5}$$

where φ is the porosity of the soil. The above equations can be used to calculate the volume of LNAPL corresponding to measured LNAPL thicknesses in each well for a site, and integrated over the site to calculate the total volume. Because LNAPL saturation varies non-linearly with elevation above the oil/water interface, the mass of LNAPL (and soluble constituents of that LNAPL) varies non-linearly with LNAPL thickness.

It should be noted that the above distribution of LNAPL and the resultant mass and volume assumes that the water table has been stable for a time period sufficient for vertical equilibrium to be established within the LNAPL phase. Fluctuations of the water table will produce a smear zone both above the LNAPL/air interface and below the LNAPL/water interface that may greatly exceed the thickness of LNAPL in the monitoring well. In these circumstances, the volume and mass of LNAPL, as well as the thickness of the LNAPL impacted zone, will be significantly greater than calculated above.

2.2. Groundwater flux

The volumetric groundwater flux (q) below and within the LNAPL pool varies as a function of the background or regional specific discharge (q_{max}) and the water saturation. Below the LNAPL/water interface, the groundwater flux is equal to the regional specific discharge. Above the groundwater piezometric surface, or corrected water table (defined as elevation where the groundwater pressure is equal to zero), there is no horizontal groundwater flux. Between the LNAPL/water interface and the groundwater piezometric surface, the groundwater specific discharge is given by:

$$q = k_{rw} k_i \frac{\rho_w g}{\mu} i \tag{6}$$

where k_{rw} is the relative permeability of the wetting phase (water), k_i is the intrinsic permeability of the soil, $\rho_w g$ is the unit weight of water, is the viscosity of water, and i is

the hydraulic gradient. Recognizing that the background or regional specific discharge (q_{max}) is simply given by:

$$q_{max} = k_i \frac{\rho_w g}{\mu} i \tag{7}$$

Eq. (6) can be rewritten as $q = k_{rw} q_{max}$, or $q/q_{max} = k_{rw}$, where the relative permeability, k_{rw}, is given by:

$$k_{rw} = S_{e_w}^{1/2}[1 - (1 - S_{e_w}^{1/m})^m]^2 \tag{8}$$

where $m = 1 - 1/n$, n is the Van Genuchten fitting parameter n, and

$$S_{e_w} = \frac{S_w - S_r}{1 - S_r}.$$

The above equations can be used to calculate the ratio of groundwater flux (q) to the regional groundwater flux (q_{max}) as a function of height above the LNAPL/water interface (Fig. 3). As mentioned, the groundwater flux below the LNAPL/water interface is equal to the regional flux ($q/q_{max} = 1.0$). Above, the LNAPL/water interface, however, the groundwater flux decreases with increasing height above the interface, as a function of decreasing water saturations. This effect is more pronounced in coarse-grained soils than in fine-grained soils because more product occupies the pore space in coarser soil for the same observed thickness (Fig. 2). Regardless of soil properties, the thickness of LNAPL in a well, or assumptions of vertical equilibrium, where LNAPL saturation is high, the relative flux of groundwater through that interval will be low.

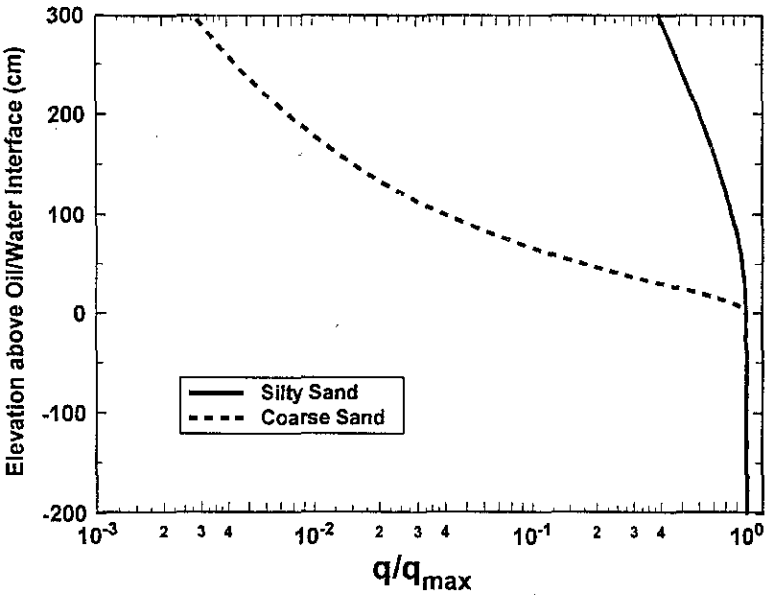

Fig. 3. Relative groundwater flux (specific discharge) above and below LNAPL/water interface.

2.3. Soluble constituent concentration

Above the LNAPL/water interface, groundwater flowing through the soil is in direct contact with LNAPL, so the concentration of a soluble constituent in a multi-component LNAPL is simply given by an analogy to Raoult's Law:

$$C_{\mathrm{eff}_m} = x_m C_{\mathrm{sol}_m} \tag{9}$$

where C_{eff_m} is the effective solubility of the m phase, x_m is the mole fraction of the m phase, and C_{sol_m} is the pure phase solubility of phase m.

Below the LNAPL/water interface, the concentration is controlled by vertical downward diffusion of the soluble constituent. This process is discussed extensively by Johnson and Pankow (1992), which, in turn, is based on the work of Hunt et al. (1988). These authors show that the concentration (C) above a DNAPL pool (or analogously below an LNAPL pool) is given by:

$$\frac{C}{C_{\mathrm{eff}}} = \mathrm{erfc}\left(\frac{z}{2\left(\frac{D_v L_p}{\bar{v}}\right)^{1/2}}\right) \tag{10}$$

where z is the distance below the LNAPL/water interface, L_p is the length of the pool along the groundwater flow direction, $\bar{v}$ is the groundwater flow velocity ($=q/\varphi_e$), φ_e is the effective porosity, and D_v is the vertical dispersion coefficient, given by $D_v = D_e + \bar{v}\alpha_v$, where D_e is the effective molecular diffusion coefficient, and α_v is the vertical dispersivity. Substitution of a wide range of velocities into this equation for an example LNAPL pool length of 10 m results in the observation that, except for the very lowest velocity (0.001 m/day or 0.36 m/year), significant concentrations are limited to a zone within 200 cm of the bottom of the LNAPL pool (Fig. 4).

2.4. Mass flux

The above calculations of soluble phase concentration distribution (Fig. 4) can be combined with the calculated groundwater flux (Fig. 3), resulting in the mass flux distribution, by noting that the mass flux (j) is given by:

$$j = qC \tag{11}$$

This soluble mass flux can be normalized to the maximum mass flux, which is simply the product of the regional specific discharge (q_{max}) multiplied by the effective solubility of the constituent of concern (C_{eff}). The result (Fig. 5) is interesting, in that it shows that:

(1) Peak mass flux occurs at the LNAPL/water interface, where the dissolved-phase concentration is equal to the effective solubility and the groundwater flux is equal to the regional flux. Above and below the interface, the mass flux decreases rapidly.

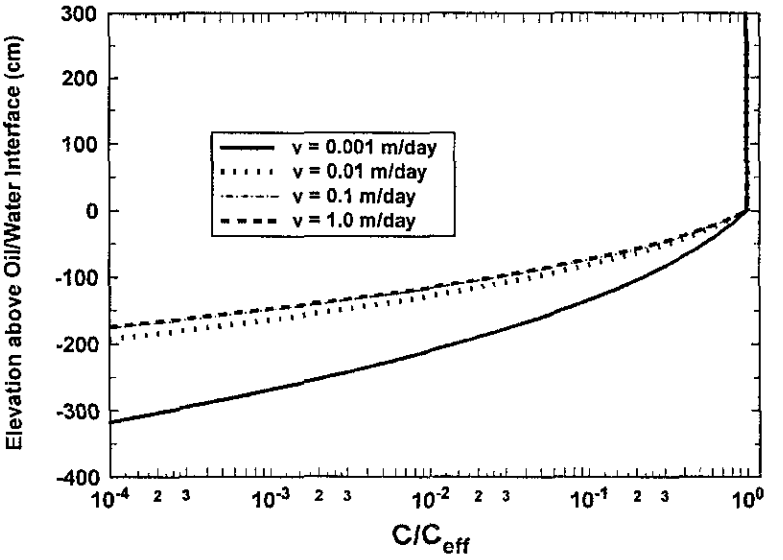

Fig. 4. Relative concentration of soluble constituents as a function of height above LNAPL/water interface.

Below the interface, the mass flux decreases because the concentration decreases away from the oil/water interface (while the groundwater flux remains constant); above the interface, the mass flux decreases as the relative permeability and groundwater flux decreases (while the concentration remains constant vertically).

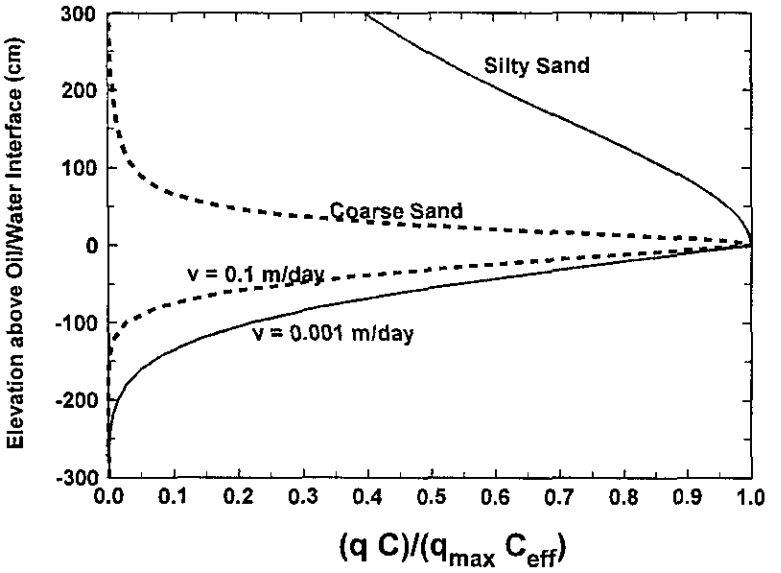

Fig. 5. Relative mass flux as a function of height above LNAPL/water interface.

(2) For most cases, the mass flux above the LNAPL/water interface (associated with groundwater flow through the LNAPL) is of the same magnitude or greater than that below the interface.

(3) Except for the lowest groundwater velocities, most of the mass flux below the LNAPL/water interface occurs within 100 cm of the interface.

(4) For coarse-grained soils, significant mass flux above the LNAPL/water interface is limited to a zone within 100 cm of the interface.

(5) For fine-grained soils, the mass flux above the LNAPL/water interface is much greater than that below, and can potentially continue to heights of more than 300 cm above the interface.

The total mass flux depleting the LNAPL source by dissolution is simply the vertical integral of Eq. (11) multiplied by a unit width of the pool. Above the LNAPL/water interface, the concentration of the soluble phase is constant with height, so the total mass flux (J_1) per unit width of LNAPL pool is given as:

$$J_1 = C_{\text{eff}} \int_0^{z_{\text{wt}}} q(z)\mathrm{d}z \tag{12}$$

where z_{wt} is the elevation of the groundwater piezometric surface (or corrected water table).

Because the water saturation profile, and therefore the relative permeability profile, cannot be integrated analytically, Eq. (12) must be numerically evaluated. Below the LNAPL/water interface, as noted above, the groundwater flux (q) remains constant while the concentration varies. Thus, the total mass flux below the interface (J_2) is given as:

$$J_2 = q \int_{-\infty}^{0} C(z)\mathrm{d}z \tag{13}$$

The distribution of concentration as a function of depth below the LNAPL/water interface is given by Eq. (10) and can be integrated analytically, resulting in:

$$J_2 = C_{\text{eff}} \sqrt{4 D_{\text{v}} q \varphi L_{\text{p}} / \pi} \tag{14}$$

The total mass flux is simply the sum of the flux above (Eq. (12)) and below (Eq. (14)) the LNAPL/water interface. For a multi-component LNAPL, such as gasoline, as each soluble component is depleted by dissolution, the mole fraction (x_m) of that component decreases, resulting in a decrease in the effective solubility of that component by Eq. (9). The implication of this is that the dissolved-phase concentration of the constituent of concern at the downgradient edge of the LNAPL pool decreases with time, thereby decreasing the mass flux into the dissolved phase which, in turn, causes contraction of the dissolved-phase plume. It is this decrease in the effective solubility of dissolved constituents of concern that we wish to examine as a measure of the persistence of the LNAPL source.

2.5. Volatilization

The mass flux (loss) due to volatilization of LNAPL components can be calculated using Fick's Law for steady-state vapor transport:

$$J_v = -D_e \frac{dC}{dZ} \tag{15}$$

where J_v is the vapor flux from the top of the LNAPL to the land surface, D_e is the effective vapor diffusion coefficient, and dC/dZ is the vapor concentration gradient. As in the water phase, Raoult's Law for the gas phase may be written as:

$$C_{veff} = \frac{x_m VP_m MW_m}{RT} \tag{16}$$

where C_{veff} is the effective vapor concentration (mg/l) of component m, VP_m is the pure phase vapor pressure of that component, MW_m is the molecular weight of the pure component, R is the ideal gas constant (0.0821 mol l/atm), and T is temperature (K). The concentration is taken to be zero at the land surface, though biodegradation often decreases the vapor phase concentration to zero below the land surface. The air diffusion coefficient can be calculated using the Millington–Quirk equation:

$$D_e = D_a \frac{\theta_\alpha^{3.33}}{\theta_t^2} \tag{17}$$

where D_a is the free-air diffusion coefficient, θ_α is the air-filled porosity, and θ_t is the total porosity (Millington and Quirk, 1961). Because the effective vapor diffusion coefficient is a function of the air-filled porosity, which varies with LNAPL and water saturations (Eqs. (3) and (4)), it varies significantly with height above the LNAPL. Therefore, an average vertical effective vapor diffusion coefficient must be used in Fick's Law. This average vertical effective vapor diffusion coefficient can be calculated in the same manner as the average vertical hydraulic conductivity of a vertically stratified sediment, which gives:

$$\overline{D_e} = \frac{\sum Z_i}{\sum Z_i / D_i} \tag{18}$$

where D_i is the diffusion coefficient of the ith interval above the top of the LNAPL and Z_i is the thickness of the ith interval. The use of an average effective vapor diffusion coefficient, calculated using the equation above, conserves mass by maintaining a constant vapor flux throughout the vertical interval.

3. Implementation

The above equations allow us to calculate the original mass of each component of the LNAPL of interest and the mass flux (loss) through both dissolution and volatilization. These calculations are all analytic, so can be implemented in a spreadsheet or by hand. However, to provide readily available implementation, we have coded the above equations into a screening tool for the American Petroleum Institute, called API-LNAST (*LN*APL

Dissolution and Transport Screening Tool; http://www.api.org/groundwater/LNAST/). This tool uses the mass flux from dissolution and (optionally) volatilization to calculate the new mass fraction of each component as a function of time. Raoult's Law (Eq. (9)) is then used to calculate the effective solubility at each time step, which changes as a function of changing mole fraction. As depletion of the LNAPL continues, the concentrations in the source area are used as time-varying input to the Domenico equation (1987), which describes the downgradient dissolved-phase concentrations as a function of the source area concentration, the groundwater flow velocity, the lateral and transverse dispersivities of the soil, the sorption characteristics of the soil and solutes, and the biodegradation rates of the solutes. The initial LNAPL distribution can be calculated in the screening tool assuming a thickness of free-phase LNAPL in a monitoring well and equilibrium distribution (Eqs. (1)–(4)), assuming LNAPL at residual saturation, assuming a user-input distribution, or can be calculated following a prescribed period of free-product recovery. Rates of LNAPL recovery from a variety of systems are calculated using the approaches of Charbeneau et al. (1999).

For the purposes of this paper, a series of calculations of the dissolution history of a simple gasoline was used to illustrate the effects of soil texture, LNAPL thickness, and remediation. The gasoline was taken to have initial mole fractions of MTBE, benzene, ethylbenzene, toluene, and xylene of 0.11, 0.018, 0.018, 0.079, and 0.075, respectively, which are typical concentrations expected at the pump, though not necessarily those found after subsurface transport of the LNAPL through the vadose zone. The gasoline was assumed to have a relative density of 0.73 and oil/water and oil/air interfacial tensions of 52 and 24 dyn/cm, respectively, representative of unweathered gasoline (Lenhard and Parker, 1990). Lower interfacial tensions are often measured as gasoline ages, resulting in somewhat greater LNAPL saturations for the same thickness.

The example geometry of the gasoline source area was 10 m long (in the direction of groundwater flow) by 5 m wide for all of the calculations, with the depth to LNAPL at 10 m from the land surface. The width of the LNAPL source area has only minimal effect on the results, but the longevity of the LNAPL is proportional to the length of the source area. The thickness of gasoline in the monitoring well was varied from 0.1 to 3 m for the calculations to derive comparative LNAPL saturation profiles for the calculations. For the calculations of reduced mass due to free-product recovery, a simple water/gasoline fluid

Table 1
Physical properties of soils used in screening tool for analysis of remediation benefit

Physical property or condition	Coarse sand	Fine sand	Silty sand
Hydraulic conductivity (m/day)	25	1	0.25
Van Genuchten α (1/m)	25	7.5	3.6
Van Genuchten n	2.8	1.9	1.6
Residual water saturation	0.04	0.15	0.19
Residual NAPL saturation	0.1	0.14	0.16
Hydraulic gradient	0.001	0.0125	0.025
Effective porosity	0.384	0.34	0.35
Longitudinal dispersivity (m)	3	3	3
Horizontal transverse dispersivity (m)	0.15	0.15	0.15

Soil capillary properties from Mualem (1976).

extraction system was assumed to operate to the point of minimal return, the ultimate endpoint of which is the residual saturation of LNAPL for that soil.

This approach was applied for a number of soil types and LNAPL thicknesses to provide some general guidance as to the longevity of the LNAPL source under conditions of both natural attenuation and free-product recovery. For this exercise, three soils were examined, a coarse sand, a fine sand, and a silty sand. The most important physical properties of each soil are summarized in Table 1. The parameters have high variability within soil types and should not be misconstrued as representative for all similar soils.

4. Results and implications

As documented in numerous laboratory experiments of multi-component dissolution, the different components of gasoline (or any multi-component mixture) are dissolved from the LNAPL source at different rates, based on their effective solubility (Fig. 6). For the gasoline composition described above, MTBE comes out of solution most rapidly, followed by benzene, with dissolution of ethylbenzene, toluene, and xylene at much later times due to their low effective solubilities.

As will be seen, a number of risk indicators, such as the concentration history at a receptor and the downgradient size of the dissolved-phase plume, are different for biodegradable and nonbiodegradable contaminants. The remainder of this discussion will focus on benzene as a representative biodegradable constituent and MTBE as representative of a minimally degradable constituent. For the purposes of the calculations, the degradation half-life of benzene was taken to be 90 days (Howard et al., 1991; Weidemeier et al., 1996) and that of MTBE was taken to be

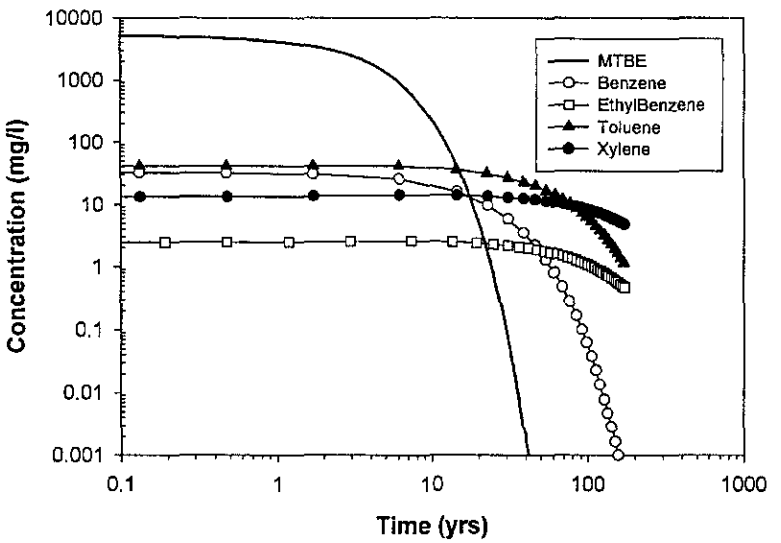

Fig. 6. Source area concentrations from dissolution of 1 m of gasoline in a coarse sand.

effectively nonbiodegrading). The half-life is a sensitive parameter, and some studies suggest that MTBE is degraded at higher rates under certain conditions (Schirmer and Barker, 1998). The values selected are intended to show the potential contrasts between refractory and non-refractory compounds, not to suggest biodegradation standards.

4.1. Biodegradable LNAPL components

4.1.1. Source area concentrations

The theoretical discussion of LNAPL depletion makes it clear that the original mass of soluble constituents will be a function of the mass and distribution of LNAPL in the soil. In our case, the thickness of LNAPL in monitoring wells and the capillary characteristics of the soils were used to calculate the resulting mass and distribution under vertical equilibrium conditions. Similarly, the depletion of the soluble fraction will be a function of the rate of the regional specific discharge and the mass and distribution of LNAPL within the soil, again calculated using the thickness of LNAPL in monitoring wells and the capillary characteristics of the soil. Log-log plots of source area concentration of benzene (Figs. 7 and 8) show a significant period where concentrations are relatively constant or decreasing only very slowly, followed by a period of relatively sharp decreases in concentration as the source area is depleted. Comparison of the dissolution histories for different LNAPL thicknesses (Figs. 7 and 8) demonstrates that increasing LNAPL thickness results in significantly increased source area longevities. This is related to the earlier observations that (1) the mass of a LNAPL increases non-linearly with the thickness of LNAPL in a monitoring well, and (2) an increase in LNAPL thickness does not greatly increase groundwater flux through the source area due to the decrease in the relative permeability of the water phase as LNAPL saturations increase. For the coarse-grained soil

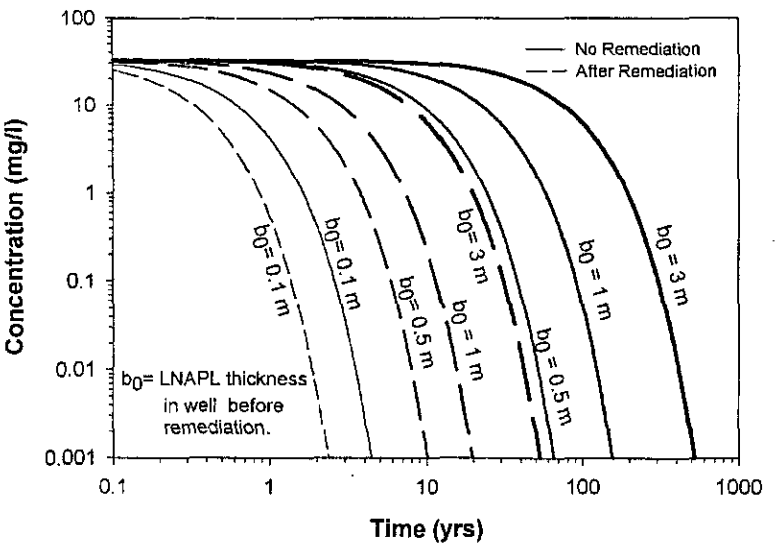

Fig. 7. Effect of LNAPL thickness and remediation on source area benzene concentrations in coarse sand.

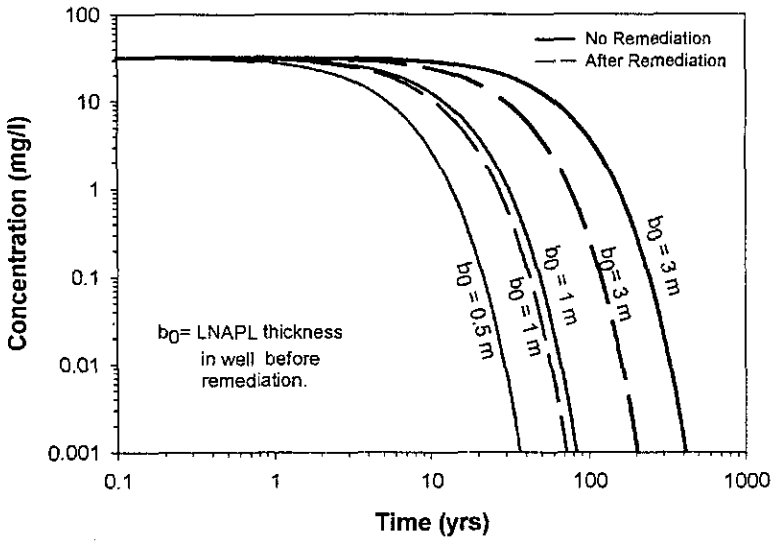

Fig. 8. Effect of LNAPL thickness and remediation on source area benzene concentrations in silty sand.

(Fig. 7), the concentration of benzene in a 10-cm-thick gasoline pool decreases immediately and reaches 1 μg/l in less than 3 years. In contrast, a 300-cm-thick gasoline pool maintains high benzene concentration for periods approaching 100 years, and persists above 1 μg/l for 500 years.

The relation between LNAPL longevity and sediment texture is a complex one. In the example chosen (Table 1; Figs. 7 and 8), the concentration histories of benzene are similar for the coarse sand and the silty sand in the unremediated cases, despite the fact that the groundwater specific discharge (q) is about four times as great in the coarse sand ($q=9$ m/year) than in the silty sand ($q=2$ m/year). For the same specific discharge and LNAPL thickness, the source area will have a much greater longevity in coarse-grained soils than in fine-grained soils, because the capillary characteristics of coarse-grained soils allow much higher LNAPL saturations than those of fine-grained soils (Fig. 2). These higher LNAPL saturations both increase the mass of the LNAPL and decrease the relative permeability of the water phase (Fig. 3), thereby decreasing the rate of dissolution.

In contrast to this, in a setting where the hydraulic gradient is the same for fine- and coarse-grained soils, such as a horizontally stratified section of sediments, the specific discharge will be much higher in the coarse-grained soil than in a fine-grained soil, due to the much higher intrinsic permeability. Here, dissolution of LNAPL from the coarse-grained soil may proceed quite rapidly, leaving most of the mass in the fine-grained soil.

For coarse sand, free-product removal results in a significant decrease in the time period when concentrations of benzene exceed 1 μg/l for almost any thickness of gasoline in a monitoring well. Applying remediation to a site with 3 m of gasoline results in removal of nearly 90% of the LNAPL and, as a result, decreases the longevity of benzene in the source area from 530 to 53 years, an order of magnitude reduction (Fig. 7). Even with only 0.1 m of gasoline in a well, remediation is estimated to remove nearly 50% of the LNAPL,

reducing benzene longevity from 4.4 to 2.4 years. As we look at increasingly finer soils, we see that the benefit of remediation decreases, particularly for smaller thicknesses of gasoline in wells. For a silty sand (Fig. 8), remediation removes about 50% of the LNAPL, reducing the longevity of benzene from 400 to 200 years, when there is 3 m of gasoline in a well—a significant decrease. However, large times are needed to dissolve and volatilize benzene even after remediation. When there is 1 m of gasoline in a silty sand, remediation removes only 13% of the LNAPL, resulting in only a minor decrease in longevity of benzene (Fig. 8). Remediation results in no LNAPL recovery and no decrease in source area longevity for 0.5 and 0.1 m of gasoline in a well in a silty sand (Fig. 8). It can therefore be seen that the apparent benefit of remediation through free-product recovery is very much a function of the soil type and the thickness of LNAPL in a well. The apparent benefit decreases with decreasing thickness of LNAPL and with decreasing grain-size (pore size). Because the effectiveness of remediation by free-product recovery, under the best circumstances, is limited by the residual hydrocarbon saturation, the difference between the initial hydrocarbon saturation and the residual hydrocarbon saturation is what really determines the effectiveness of remediation in terms of reducing the longevity of any component. As this difference is typically much smaller in fine-grained soils than in coarse, resulting in a smaller percentage decrease in mass in fine-grained soils, remediation in fine-grained soils is much less effective in decreasing the longevity of the LNAPL as a source of dissolved-phase solutes. If groundwater production rates are too high during remediation, the LNAPL may be smeared out over a thicker interval, resulting in even higher residual LNAPL mass (Beckett and Huntley, 1998). The effect on source area longevity, however, is not obvious, as dissolution rates are also increased due to the increased thickness of the LNAPL-impacted interval.

Another measure of the benefit of remediation is the corresponding reduction in risk. Risk is typically defined at specific receptors and is a function of concentration and duration of a contaminant, such as benzene, at that receptor. Therefore, one might look at two separate measures of risk, the maximum downgradient extent of a dissolved-phase plume (defined as the maximum distance at any time where concentrations exceed a target), and the concentration–time profile at a specific receptor.

4.1.2. Extent of plume

The predicted evolution of a dissolved-phase plume, as described in the introduction to this paper, can be seen in the results from the screening tool for the coarse sand (Fig. 9). For example, for 3 m of gasoline in a coarse sand, the benzene plume expands to a maximum distance of about 45 m over the first 4 years after initial contact between the gasoline and the water table. The plume then remains stable for about 30 to 40 years, followed by a slow contraction of the plume. With the exception of the 0.1 m result, the thickness, and therefore the mass, of the LNAPL does not have a large influence over the maximum downgradient extent of the dissolved-phase plume, but does have a significant effect on the time period before contraction of the plume is seen. For example, the maximum extent of the dissolved-phase plume corresponding to a 0.5-m LNAPL thickness at the source is about 40 m, which increases only to 45 m when the LNAPL thickness at the source area is increased to 3 m. However, the dissolved-phase plume starts contracting almost immediately for LNAPL thicknesses of 0.5 m or less, whereas it takes

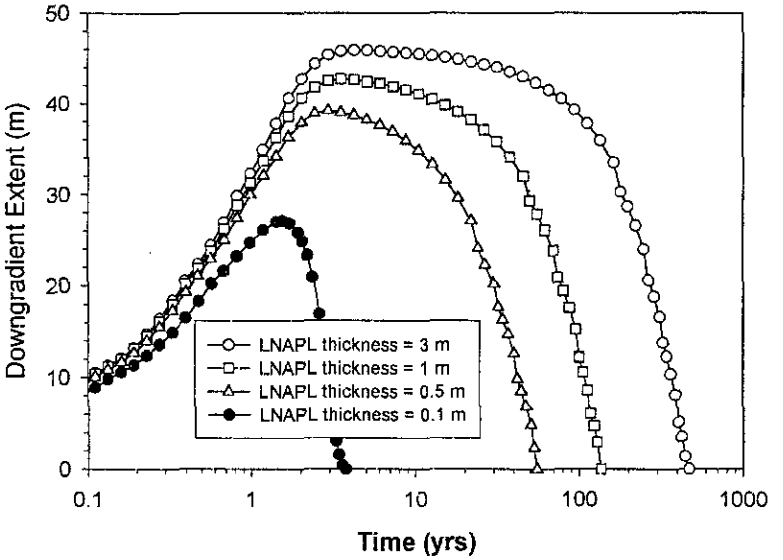

Fig. 9. Effect of LNAPL thickness on downgradient extent of benzene plume, coarse sand.

about 30 years to see contraction of the dissolved-phase plume when the LNAPL is 3 m thick. The same conclusion can be drawn when comparing soils with different capillary characteristics, which affect LNAPL mass in a manner similar to LNAPL thickness. In fact, for a one-dimensional flow and solute transport field, with no dispersion, the maximum downgradient extent of the plume (d) can be calculated simply as:

$$d = t\frac{q}{\varphi_e} \tag{19}$$

where t is the time that a biodegradable constituent is reduced from its initial concentration (C_0) to its target concentration (C), given by:

$$t = \frac{1}{\lambda}\ln\left(\frac{C_0}{C}\right) \tag{20}$$

where λ is the decay coefficient, which, in turn, is given by:

$$\lambda = \frac{\ln(2)}{t_{1/2}} \tag{21}$$

where $t_{1/2}$ is the half-life of the biodegradable constituent. Based on this analysis, the maximum downgradient extent will be linearly proportional to the groundwater flow velocity (q/φ_e) and inversely proportional to the biodegradation decay coefficient. It should be pointed out, however, that biodegradation rates and groundwater flow velocities may not be independent. For a fixed electron acceptor concentration, such as oxygen,

increases in groundwater flow velocities will increase the mass flux of electron acceptors into the dissolved-phase plume and therefore increase the rate of biodegradation.

The effect of remediation, resulting in a reduction in the mass of gasoline in the soil, is a more rapid contraction of the dissolved-phase plume, without significantly changing the maximum downgradient extent of the dissolved-phase plume. This can be seen for both the 3-m thickness and the 1-m thickness of gasoline in the coarse sand (Fig. 10), where the maximum downgradient extent is 45 m, whether the site is remediated or not. After 10 years, however, the dissolved-phase plume downgradient of the remediated source area is significantly smaller than that downgradient of the non-remediated source. For the silty sand (not shown), the effects of remediation of the source area for both 3 m and 1 m of gasoline in a well are negligible, as measured by the downgradient extent of the benzene plume.

4.1.3. Concentration–time profiles

Remediation affects the concentration–time profile in a manner similar to the effect on the extent of the plume. A reduction in the LNAPL saturation does not impact the maximum concentration seen at a specific receptor (well), but causes a more rapid decrease in concentration and decrease in the area under the concentration vs. time curve. For example, for 3 m of gasoline in a coarse sand (Fig. 11), the maximum concentration in a monitoring well 15 m downgradient from the source is predicted to be about 2 mg/l, whether the site is remediated or not. However, remediation produces much more rapid depletion of benzene from the source, resulting in rapid decreases in benzene concentration in less than 30 years, compared to the very slow decline in

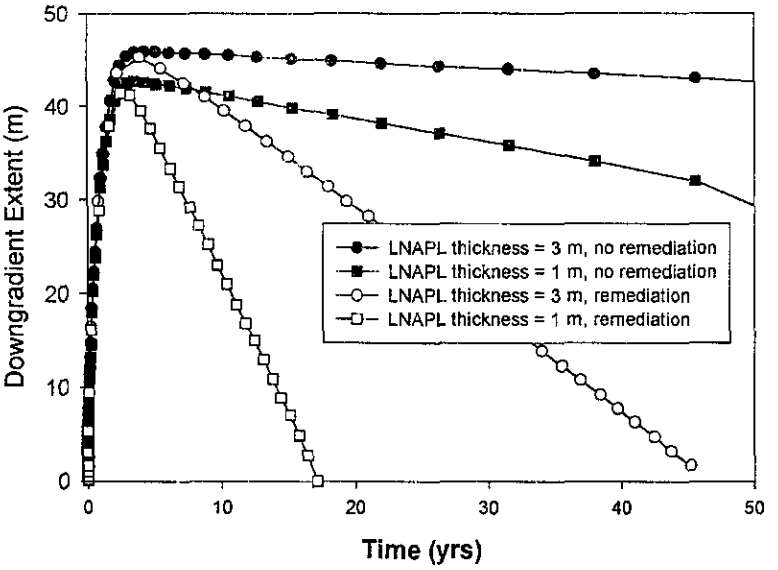

Fig. 10. Effect of remediation on downgradient extent of dissolved-phase benzene plume, coarse sand.

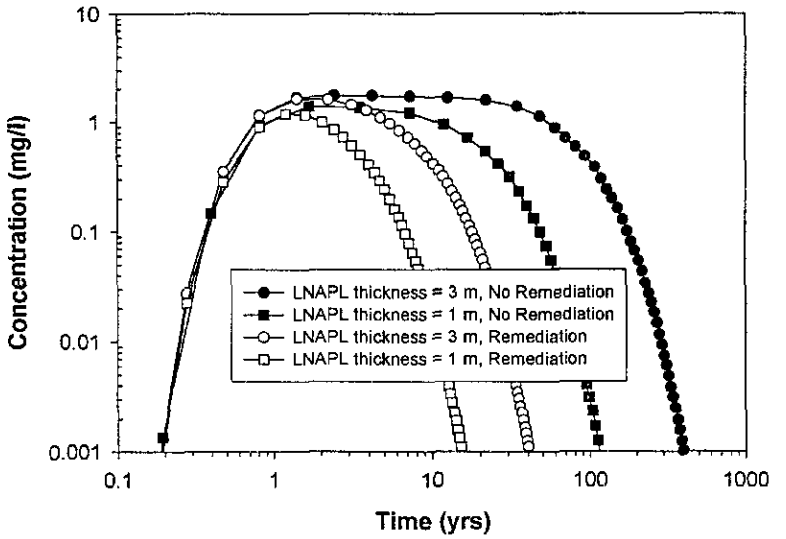

Fig. 11. Effect of remediation on benzene concentration 15 m downgradient from source area, coarse sand.

concentration still seen 100 years after the gasoline came in contact with groundwater. As in other analyses, the effect of remediation in the silty sand (not shown) is minor, even for 3 m of gasoline.

4.2. Nonbiodegradable compounds

The effects of free-product recovery on MTBE concentrations in the source area are similar to the effects already described for benzene, except that MTBE is depleted from the source more rapidly than benzene (Fig. 6) for both remediated and non-remediated conditions. A substantial difference, however, is seen in the maximum downgradient extent of biodegradable and nonbiodegradable compounds. Whereas the maximum extent of the dissolved-phase benzene plume is unaffected by remediation (Fig. 10), the maximum downgradient extent of the MTBE plume decreases significantly (from 1100 to 600 m) through remediation for the coarse sand (Fig. 12). Similar benefits for fine-grained soils, such as a silty sand, are not observed.

This difference between the response of benzene (Fig. 10) and MTBE (Fig. 12) is observed because the maximum downgradient extent of biodegradable compounds such as benzene is established by the equilibrium between mass flux from the source area and biodegradation rate. When biodegradation rates are low, as was assumed for MTBE, the plume continues to spread downgradient until the source is depleted, and for some time after. This points out the critical importance of the biodegradation rate selected for evaluations.

The benefits of remediation on the concentration–time profiles at specific receptors for nonbiodegradable compounds are similar to those benefits discussed for degradable constituents.

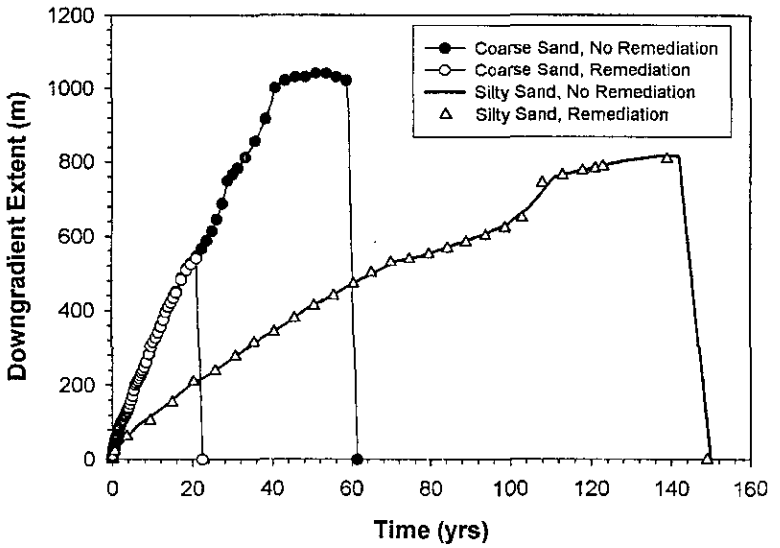

Fig. 12. Effect of remediation on downgradient extent of dissolved-phase MTBE plume, coarse sand and silty sand. Initial LNAPL thickness was 1 m for both soils.

4.3. Alternate remediation approaches

The limited benefit of free-product recovery on the extent, duration, or concentrations within the dissolved-phase plume for fine-grained soils, such as the silty sand discussed above, is disappointing. Our work, however, suggests that alternate technologies, such as air sparging or vapor extraction that target the more volatile constituents within the LNAPL without removing large masses of the LNAPL, may be more effective at reducing concentration in these finer-grained soils, as long as the cleanup mechanism is delivered efficiently to the LNAPL zone. For example, consider the results discussed above for the silty sand with 1 m of gasoline in wells. Free-product recovery resulted in minimal decrease in the longevity of benzene in the source area, no significant decrease in the maximum downgradient extent of the benzene plume, and no significant decrease in the peak concentration at a receptor 5 m downgradient from the source or real decrease in the integral of the concentration–time function. If we compare this to the result of a technology that reduces the mole fraction of the benzene in the gasoline from 0.018 to 0.0018 and the mole fraction of the MTBE from 0.11 to 0.011, we see some real differences. Post-remediation concentrations of both benzene and MTBE are predictably lower in the source area at early times (Fig. 13). However, because dissolution rates decrease with decreasing mole fraction, a 90% reduction in mass does not result in a 90% decrease in the time that each compound exceeds a target concentration. Reducing the MTBE mole fraction from 0.11 to 0.011 (Fig. 13) is similar to the effects of the first four years of dissolution of a gasoline with a 0.11 mol fraction of MTBE, which decreases the time to reduce the concentration of MTBE in the source area to the target concentration from 23 fto 19 years.

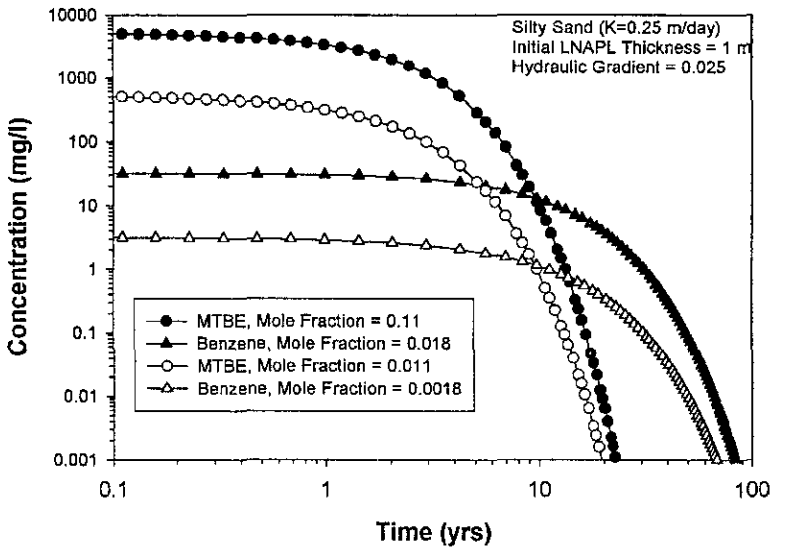

Fig. 13. Effect of a reduction in mole fraction on MTBE and benzene concentrations in source area, silty sand.

The real differences, however, are seen in the downgradient extent of the dissolved-phase plumes and the concentrations at receptors (Figs. 14 and 15). A decrease in the mole fraction of benzene reduces the maximum downgradient extent from 19 to 14 m

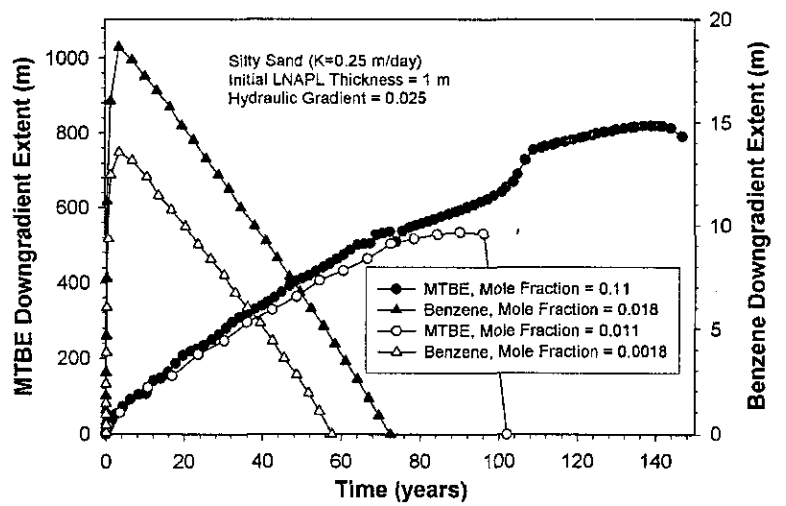

Fig. 14. Effect of a reduction in mole fraction on extent of MTBE and benzene dissolved-phase plumes, silty sand.

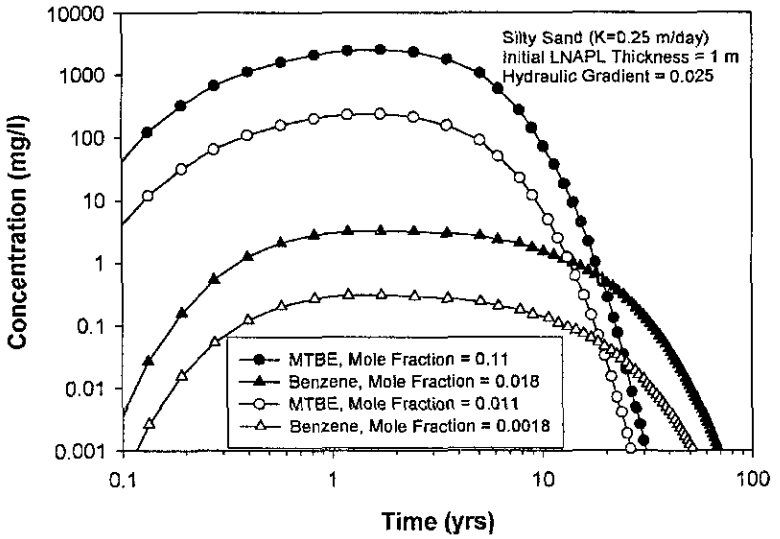

Fig. 15. Effect of a reduction in mole fraction on MTBE and benzene concentrations 5 m downgradient of source area, silty sand.

(Fig. 14) and reduces the peak concentration seen at a receptor 5 m downgradient from the source from 2 to 0.2 mg/l (Fig. 15). Similarly, reduction of the mole fraction of MTBE results in a decrease in the maximum downgradient extent from 800 to 500 m and a reduction in peak concentration at a receptor 5 m downgradient from the source from 2000 to 200 mg/l (Fig. 15).

5. Summary and conclusions

We have provided an approach, based on a series of analytic solutions, to assess the changing concentration and mass flux of a soluble component at the downgradient edge of a multi-component LNAPL pool. The analytic solutions used in this analysis are those that govern the distribution of LNAPL saturations in an LNAPL/water system, the relation between water saturations and the relative permeability of the wetting (water) phase, the relation between dissolved-phase concentration and the depth below an LNAPL pool, and the relation between effective solubility of a component in a multi-component LNAPL mixture and the mole fraction of that component. The results of this exercise demonstrate that:

(1) Groundwater flow through the LNAPL pool is at least as important to the dissolution process as dissolution below the pool. This dissolution accompanying flow through the LNAPL pool has been ignored in previous work describing dissolution of NAPL, except where LNAPL saturations approach residual.

(2) For a 10-m-long gasoline pool, the effective solubility of benzene remains above 1 μg/l for periods exceeding 30 to 100 years for all but (a) very thin (0.1 to 0.5 m) pools, (b)

fine-grained soils with low LNAPL saturations (but only when significant groundwater flux is maintained), or (c) very high groundwater fluxes.

(3) For biodegradable constituents, the maximum downgradient extent of the dissolved-phase plume is largely unrelated to the LNAPL mass, as controlled by pool thickness or soil capillary properties. Instead, the downgradient extent is controlled by the relation between the mass flux from the source area, the groundwater flow velocity, and the rate of biodegradation.

The above results are consistent with the statistical observations of Rice et al. (1995) and explain a number of anecdotal observations reported by consultants and regulators alike. Noted at the beginning of this paper was the concern voiced by many regulators that most dissolved-phase plumes downgradient from LNAPL sources appeared to be maintaining a relatively constant size, with very few expanding. This is consistent with the observation that the time to reach a relatively constant size is limited entirely by the biodegradation rate. Using benzene as an example, with a reported half-life of 30 to 90 days, the time for the soluble fraction to decay from 54 mg/l to 1 μg/l varies from 1.3 to 3.9 years. Therefore, any spill which is older than this will have already reached its maximum extent. Further, our analysis of the depletion of LNAPL sources shows that, for situations other than very thin LNAPL pools, it will typically take periods of more than 30 years to see significant depletion of benzene from the source area, resulting in contraction of the dissolved-phase plume. This is again consistent with the analysis of Rice et al. (1995), where only 33% of the benzene plumes were contracting, despite the fact that half of the sites included in the study showed less than 3 cm of hydrocarbon.

Our analysis also indicates that, contrary to what is commonly assumed, recovery of LNAPL by liquid pumping is often ineffective at managing or reducing concentration. Except in coarse soils or medium-grained soils with high LNAPL saturations, remediation by free-product recovery approaches does not result in significant reductions in the longevity of downgradient dissolved-phase contamination. Further, for biodegradable constituents, remediation does not result in a decrease in the maximum downgradient extent of contamination, which is almost solely related to groundwater velocities and biodegradation rates. However, for those soils where the initial LNAPL saturation is significantly above the residual LNAPL saturation, free-product recovery does result in more rapid contraction of the dissolved-phase plume. Cleanup methods that act to change the composition of the LNAPL source, by reducing the mole fraction (and therefore the mass and effective solubility) of constituents of concern are much more effective at reducing both the concentration at downgradient receptors and reducing the maximum downgradient extent of both degradable and nondegradable compounds, particularly for fine-grained soils or when LNAPL saturation is low.

Acknowledgements

A portion of this work was funded by the American Petroleum Institute. The authors would like to thank the reviewers of this paper for their very helpful comments.

References

Beckett, G.D., Huntley, D., 1998. Soil properties and design factors influencing free-phase hydrocarbon recovery. Environmental Science and Technology 32, 287–293.

Charbeneau, R.R.J., Lake, L., McAdams, M., 1999. Free-product recovery of petroleum hydrocarbon liquids. API Publication, vol. 4682. American Petroleum Institute, Washington, DC.

Domenico, P.A., 1987. An analytical model for multidimensional transport of a decaying contaminant species. Journal of Hydrology 91, 49–58.

Farr, A.M., Houghtalen, R.J., McWhorter, D.B., 1990. Volume estimation of light nonaqueous phase liquids in porous media. Ground Water 28, 48–56.

Johnson, R.L., Pankow, J.F., 1992. Dissolution of dense chlorinated solvents in groundwater. 2. Source functions for pools of solvent. Environmental Science and Technology 26, 896–901.

Howard, P.H., Boethling, R.S., Jarvis, W.F., Meylan, W.M., Michalenko, E.M., 1991. Handbook of Environmental Degradation Rates. CRC Press, Boca Raton, FL.

Hunt, J.R., Sitar, M., Udell, K.S., 1988. Nonaqueous phase liquid transport and cleanup: 1. Analysis of mechanisms. Water Resources Research 24, 1247–1259.

Huntley, D., Hawk, R.N., Corley, H.P., 1994. Non-aqueous phase hydrocarbon in a fine-grained sandstone: 1. Comparison between measured and predicted saturations and mobility. Ground Water 32.

Lenhard, R.J., Parker, J.C., 1990. Estimation of free hydrocarbon volume from fluid levels in monitoring wells. Ground Water 28, 57–67.

Lundegard, P.D., Mudford, B.S., 1998. LNAPL volume calculation: parameter estimation by nonlinear regression of saturation profiles. Ground Water Monitoring and Remediation 18, 88–93.

Millington, R.J., Quirk, J.M., 1961. Permeability of porous solids. Transactions of the Faraday Society 57, 1200–1207.

Mualem, Y., 1976. A catalogue of the hydraulic properties of unsaturated soils. Development of methods, tools and solutions for unsaturated flow with application to watershed hydrology and other fields. Israel Institute of Technology.

Rice, D.W., Grose, R.D., Michaelsen, J.C., Dooher, B.P., MacQueen, D.H., Cullen, S.J., Kastenberg, W.E., Everett, L.G., Marino, M.G., 1995. California leaking underground fuel tank (LUFT) historical case analyses. California Environmental Protection Dept. Report UCRL-AR-122207, Sacramento, CA.

Schirmer, M., Barker, J.F., 1998. A study of long-term MTBE attenuation in the Borden aquifer, Ontario, Canada. Ground Water Monitoring and Remediation 18, 113–122.

Van Genuchten, M.Th., 1980. A closed-form equation for predicting the hydraulic conductivity of unsaturated soils. Soil Science Society of America Journal 44, 892–899.

Wiedemeier, T.H., Swanson, M.A., Wilson, J.T., Kampbell, D.H., Miller, R.N., Hansen, J.E., 1996. Approximation of biodegradation rate constants for monoaromatic hydrocarbons (BTEX) in ground water. Ground Water Monitoring and Remediation 16, 186–194.